TABLE 2

Distribution of offspring's genotypes by mating between *Impa1* Lys-95 heterozygotes

The abbreviations used are as follows: Wild, wild-type control; Het, heterozygote; and Homo, homozygote mice.

Stage		Wild	Het	Homo	Sum	χ^2 test ($df = 1$)
Standard diet during pregnancy and lactation						
E10.5	Observed	12	23	11	46	$\chi^2 = 0.0435, p = 0.83$
	Expected	11.5	23	11.5		
E14.5	Observed	9	20	7[a]	36	$\chi^2 = 0.0667, p = 0.41$
	Expected	9	18	9		
E18.5	Observed	68	136	30[a,b]	204	$\chi^2 = 18.5, p = 1.69 \times 10^{-5}$
	Expected	58.5	117	58.5		
Weaning	Observed	30	53	1	84	$\chi^2 = 25.8, p = 3.81 \times 10^{-7}$
	Expected	21	42	21		
Inositol supplementation during pregnancy and lactation						
E18.5	Observed	8	26	12	46	$\chi^2 = 1.48, p = 0.22$
	Expected	11.5	23	11.5		
Weaning	Observed	146	325	127	598	$\chi^2 = 5.73, p = 0.017$
	Expected	149.5	299	149.5		

[a] All fetuses/embryos show mandible hypoplasia.

[b] Data include one dead fetus with a normal body size and mandible hypoplasia.

C57BL/6N strain for six generations to dilute unrelated mutations on a homogeneous genetic background (Fig. 1*A*). Heterozygous males and females from the three strains were mated, and the genotypes of the offspring were determined at weaning. T95K heterozygotes grew normally (Fig. 2*D*), but only one homozygote (1/84 (1.2%)) was identified (Table 2), implying an essential role for IMPase 1 activity in survival. The lone homozygote, which was undersized and weak, died shortly after weaning (data not shown). In contrast, homozygous and F81L and T96A mice were present at the expected segregation ratio without any visible phenotypic changes (Fig. 2*D* and data not shown). We therefore focused on the *Impa1* T95K (Lys-95) strain.

To determine when Lys-95 homozygous pups die, we again intercrossed heterozygous T95K mice and determined the segregation ratios of offspring genotypes at E18.5. There were significantly fewer homozygous embryos at E18.5 than expected (30/204 (14.7%), $\chi^2, p = 1.69 \times 10^{-5}$) (Table 2). The body sizes of the surviving homozygotes (Fig. 3*A*, denoted as *Homo*) ranged from being slightly to significantly smaller than those of wild-type (denoted as *Wild*) and heterozygous (denoted as *Het*) littermates. The head to body ratio of homozygotes appeared smaller than wild-type controls (Fig. 3*A*, and data not shown). Surprisingly, the lower jaws of homozygous fetuses were abnormally shorter (mandibular micrognathia) than those of wild-type controls (Fig. 3, *A* and *B*, and data not shown), indicating aberrant craniofacial development. Moreover, homozygotes had poorly developed tongues (Fig. 3, *A* and *B*) and mandible hypoplasia, revealed by Alcian blue and alizarin red staining (Fig. 3*C*). These cranial malformations showed 100% penetrance. The severity of mandible hypoplasia did not correlate with body size (Fig. 3*A*, and data not shown), supporting the conclusion that the mandible phenotype was not a result of delayed growth. Notably, we found no clear defects in the upper jaw or palate closure of homozygotes (Fig. 3, *A* and *B*). In addition to lower jaw malformation, ~30% of homozygotes exhibited asymmetric sternum-rib fusion (Fig. 3*D*). Two homozygous pups exhibited exencephaly (data not shown), and one exhibited a cleft palate (data not shown). However, because the number of these phenotypic abnormalities was not statistically significant, we could not eliminate the possibility that the mutations were not causal. The homozygotes that survived until E18.5 stopped moving within a few minutes after Caesarean section delivery, whereas wild-type and heterozygous littermates continued to move and were resuscitated. Because abnormal peripheral neuronal development is a major cause of paralysis after delivery, we examined neural fiber formation in E10.5 embryos by whole-mount immunohistochemistry, with an anti-neurofilament antibody. We found no detectable differences in neural organization between wild-type and homozygous embryos (Fig. 4*A*). At E10.5, embryo genotypes from heterozygote intercrossing were present at the expected segregation ratios (Table 2), and there were no visible morphological abnormalities in homozygous embryos (Fig. 4*A*). These data show that the retardation in mandible formation appears slowly after E10.5 in homozygotes. To investigate this point, we examined heterozygote intercrosses at E14.5. Even at this stage, we were clearly able to discriminate homozygotes from wild-type and heterozygous littermates, based on hypoplasia of the lower jaw (Fig. 4*B*, *yellow arrowheads*) and the Meckel's cartilage (Fig. 4*B*, *red arrowheads*), which is laid down prior to mandible formation in the developmental process. We detected no evidence of biased genotype distribution in offspring at E14.5 (Table 2). Importantly, with the exception of the mandible, the gross architecture of the skull, including the maxilla, appeared to be normal (Fig. 4*B*). Collectively, these results indicate that the cause of mandible hypoplasia is most likely due to abnormal differentiation of the mandibular process from the first pharyngeal arch.

To test whether the Lys-95/Lys-95 phenotypes were caused by a reduction in cellular *myo*-inositol levels, we supplemented the drinking water of heterozygous females with 2% *myo*-inositol before mating. *myo*-Inositol supplementation, which continued until weaning (Fig. 5*A*), significantly enhanced the survival of homozygotes (127/598, 21.2%) (Table 2). The survivors showed no visible abnormalities in craniofacial development (Fig. 5, *B* and *C*) or gross brain structure (Fig. 5*D*). Moreover, we found no homozygous fetuses with malformation of the rib cage (Fig. 5*B*). Based on these lines of evidence, we postulate a direct relationship between developmental defects in homozygotes and a relative reduction of cellular *myo*-inositol. The levels of *Impa1* mRNA did not differ in various tissues among the

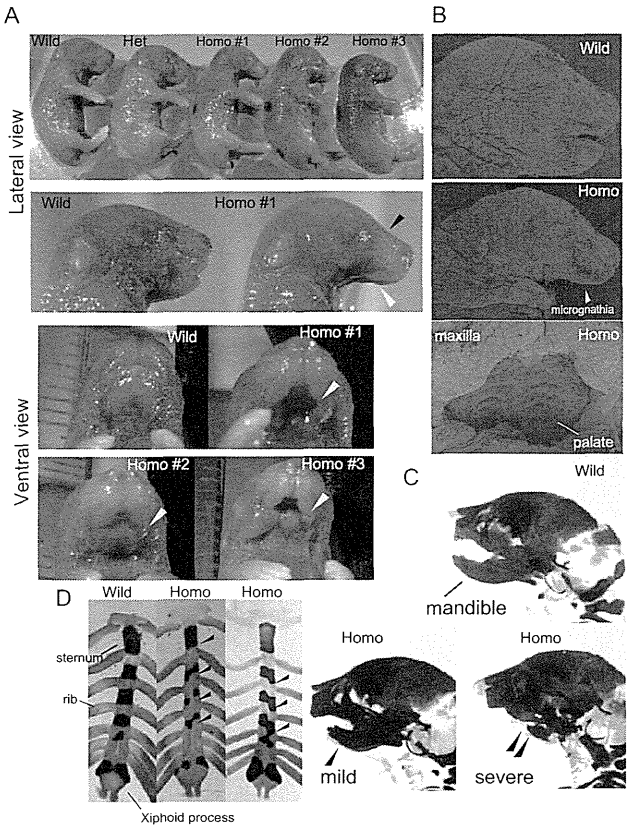

FIGURE 3. **Lys-95 homozygotes exhibit characteristic developmental defects at E18.5.** *A*, E18.5 fetuses from a single litter mating of heterozygotes are shown (*top panel*). This litter contained one wild-type (*Wild*), one heterozygote (*Het*), and three (*Homo #1–3*) homozygote (*Homo*) mice. The tips of mouse tails were removed for genotyping. Magnified lateral views of wild-type (*Wild*) and *Homo #1* fetal heads are shown in the *2nd row*. Homozygotes show incompletely developed mandibles (*yellow arrowheads*) and malformed heads (*black arrowheads*). Ventral views of wild-type, *Homo #1* (severe), *Homo #2* (mild), and *Homo #3* (moderate) mice are shown in the *bottom four panels*. Hypoplasia of the mandible (*yellow arrowheads*, micrognathia) is evident in homozygotes. *B*, scanning electron microscopic images of mouse heads. Homozygous fetuses lack most of the lower jaw and tongue (*middle*). The head of a wild-type littermate is shown at the *top*. The palate is formed in homozygotes (*bottom*). *C*, skulls of wild-type and homozygote fetuses were visualized using Alcian blue and alizarin red staining. Images show typical wild-type (*Wild*) and homozygote (*Homo*) mice, demonstrating mild and severe mandible hypoplasia. Hypoplasia is indicated by *arrowheads*. *D*, Alcian blue and alizarin red staining of rib cages. Images show typical wild-type (*Wild*) and homozygote (*Homo*) mice. Fusion of ribs to the sternum is asymmetric in E18.5 homozygotes. The bifida sternum is evident in the homozygotes. *Blue arrowheads* indicate the sites of asymmetric connection of ribs to the sternum.

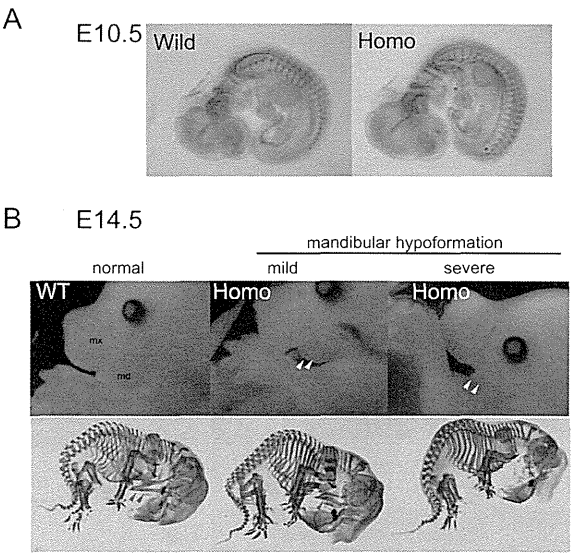

FIGURE 4. **Hypoformation of Meckel's cartilage in Lys-95 homozygotes.** *A*, neural fiber organization of an E10.5 embryo was analyzed in whole mounts by immunochemical staining (2H3, anti-neurofilament antibody). There was no apparent difference between wild-type (*Wild*) and homozygous T95K (*Homo*) littermates. *B*, homozygous embryos show hypoformation of Meckel's cartilage. Typical pictures are shown for wild-type (*Wild*) and homozygous (*Homo*) E14.5 mouse embryos. *Yellow arrowheads* indicate hypoformation of the lower jaw. Bone preparations stained by Alcian blue and alizarin red are also shown. *Red arrowheads* (Meckel's cartilage) indicate hypoformation of the lower jaw.

three genotype cohorts fed water, instead of *myo*-inositol after weaning (data not shown), indicating that the mutation had no effect on the transcription or stability of *Impa1* mRNA. Homozygotes and wild-type controls consistently expressed similar levels of IMPase 1 protein (Fig. 5*E*). Neither *Impa2* mRNA nor protein levels were elevated to compensate for deficits in IMPase 1 activity (Fig. 5*E* and data not shown). The rescued homozygotes died from unknown causes before the wild-type controls (Fig. 5*F*).

As stated earlier, IMPase 1 is the likely molecular target for lithium when used as a mood stabilizer. Therefore, we explored whether loss of IMPase 1 activity could mimic behavioral changes seen in animals given lithium, using inositol-rescued adult mice (Fig. 5*A*). We examined mice of both sexes, aged 12 weeks and older, using a comprehensive battery of behavioral tests (Table 3) covering multiple domains of the brain functionality, such as motor function, affective traits, and cognitive and sensorimotor gating functions (26–31). Many researchers have detected antidepressant-like effects for lithium when administered to rodents in various experimental paradigms, including the forced swim and tail suspension tests. Both of these are basic tests to evaluate manic or depressive moods in rodents, where the antidepressant-like effect of lithium is detected as decreased immobility time. *Impa1* T95K homozygotes of both sexes exhibited hyperactivity, collectively determined based on the following observations: 1) increased total distances traveled in the dark- and light-box test (Fig. 6*A*); 2) decreased immobility time in the forced swim test (Fig. 6*B*); 3) increased entry number in the Y-maze test (Fig. 6*C*), and 4) reduced freezing behavior on the conditioning day of the fear-conditioning test (Table 3). We also observed a significant increase in the total distance in the elevated plus-maze test and in daytime locomotor activity in the home cage for females, as well as an increased tendency for both measures in males. In addition, we detected increased locomotor activity in the open field test for males (Fig. 6*D*), whereas there were no significant differences between homozygotes and wild-type controls during the first 10 min of the open field test (Table 3 and Fig. 6*D*).

Because *Impa1* is highly expressed in mouse cerebellar Purkinje cells (8), we examined whether *Impa1* Lys-95 homozy-

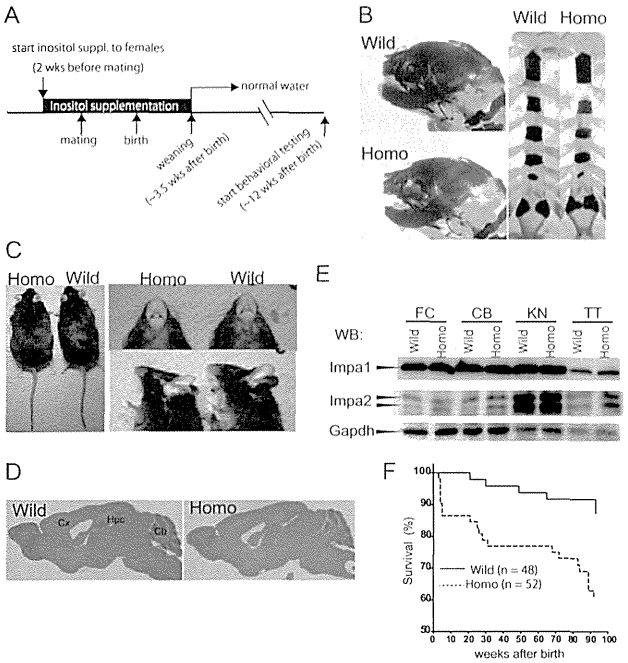

FIGURE 5. ***myo*-Inositol supplementation during pregnancy rescues the lethality and craniofacial defects of Lys-95 homozygotes.** *A*, schematic of the protocol for *myo*-inositol supplementation. *B*, Alcian blue and alizarin red staining of rib cages at E18.5. Typical pictures show wild-type (*Wild*) and homozygote (*Homo*) mice. Note that malformation of the jaw or rib cage is not visible in homozygotes. *C*, there was no gross difference between adult wild-type and homozygote mice (*left panel*). Abnormal lower jaw morphology was rescued by dietary supplementation with inositol during pregnancy (*right panels*). *Top right*, ventral view; *bottom right*, lateral view. *D*, there were no gross structural abnormalities in the brains of homozygotes stained with hematoxylin and eosin. *Cx*, cerebral cortex; *Hpc*, hippocampus; *Cb*, cerebellum. *E*, expression level of the Impa1 protein in homozygotes was comparable with that of wild-type controls. Lysates (40 μg of protein) prepared from K95/K95 and control mice were analyzed by Western blotting (*WB*) with anti-Impa1, anti-Impa2, or anti-Gapdh antibodies. *FC*, frontal cortex; *CB*, cerebellum; *KN*, kidney, and *TT*, testis. *F*, Kaplan-Meier survival analysis of mice rescued with *myo*-inositol. Homozygotes (*Homo*) showed normal morphology, but their life spans were shorter than those of wild-type (*Wild*) controls. Note that after weaning, mice drank water without *myo*-inositol.

TABLE 3

Summary of behavioral test battery of homozygotes

All the analyses were done using 8–24 mice/genotype. NS means not significant in male and female; ASR means acoustic startle response; CS means conditioned stimuli; US means unconditioned stimuli; PP means prepulse; P means pulse.

Test	Measure	Difference from wild-type control
Open field (10 min)	Total distance	NS[a]
	Center time (%)	Decreased[a,b]
Home cage activity	Total activity (/24 h)	NS[a]
	Day time (/12 h)	Increased[a,c]
	Night time (/12 h)	NS[a]
Elevated plus maze	Open stay (%)	Increased[a,b]
	Closed stay (%)	Decreased[a,b]
	Center (%)	NS[d]
	Total distance (cm)	Increased[a,c]
Light/dark transition	Light distance (cm)	NS[a]
	Dark distance (cm)	Increased[a,e]
	Total distance (cm)	Increased[a,e]
	Light time (s)	NS[a]
	Dark time (s)	NS[a]
	Entry numbers	NS[e]
	Latency to dark box (s)	Decreased[b,d]
Tail suspension	Immobility (%)	NS[a]
Forced swim	Immobility time (5 min)	Decreased[a,e]
Y maze	Alteration (%)	NS[d]
	Entry numbers	Increased[d,e]
Fear conditioning (freezing (%))	Conditioning (pre-+post-US/CS)	Decreased[d,e]
	Contextual	NS[a]
	Cued (pre-CS)	NS[d]
	Cued (post-CS)	NS[d]
Prepulse inhibition	74/120 (PP/P db) (%)	NS[f]
	80/120 (PP/P db) (%)	
	86/120 (PP/P db) (%)	
ASR	at 120 db	NS[a]

[a] Student's *t* test.
[b] Difference was detected only in males.
[c] Difference was detected only in females.
[d] Mann-Whitney's *U* test.
[e] Significant difference was detected in both sexes.
[f] Repeated measures two-way analysis of variance (genotype effect).

gotes suffered from a motor coordination deficiency. We found that performance in the rotarod test was unaffected (data not shown). Interestingly, ~5% of older homozygotes (>1.5 years) exhibited epileptic responses when removed from their home cages and placed on the floor (supplemental Movie 1). Typically they recovered within 10 min of being returned to their home cages. Taken together with the behavioral abnormalities of the *Impa1* Lys-95 homozygotes, we conclude that *Impa1*-dependent *myo*-inositol turnover plays crucial roles in the generation and maintenance of brain function integrity.

A large body of evidence demonstrates a correlation between affective disorders (including bipolar disorder and major depressive disorder) and circadian dysregulation (32, 33), represented by high comorbidity of affective disorders and sleep disturbances. To identify possible effects for the *Impa1* T95K mutation on circadian functions, we examined the properties of rest-activity rhythms of homozygotes under entrained and free-running conditions. As lithium prolongs the circadian period (τ) when administered to rodents, this period in homozygotes may be prolonged if lithium targets IMPase 1 *in vivo*. Our homozygotes showed a normal activity rhythm under regular 12-h light:12-h dark conditions (Fig. 7*A*). Interestingly, we observed that both the onset and offset (Fig. 7*B*, *red* and *blue arrowheads*, respectively) of the free-running activity rhythms of homozygotes were gradually delayed compared with that of the wild types under constant darkness (DD) (Fig. 7*B*). This trend was clearly visible between DD cycles 11 and 13 (Fig. 7*C*). We analyzed this same data set and determined the free-running circadian period, and we found that mutants showed significantly lengthened circadian periods (Fig. 7*D*). It is highly plausible that the delayed timing of activity rhythms induced by this mutation is the result of prolonged circadian periods. Importantly, a similar prolonging circadian period effect has been reported repeatedly in animals, including rodents treated with lithium, as we will discuss later.

In addition to the beneficial effects on mood, lithium therapy frequently causes multiple side effects, including poisoning, making it essential to monitor and control lithium serum concentrations. Some undesirable effects of lithium can potentially be mediated by inhibiting IMPase. The typical side effects of lithium therapy, including tremor and polyuria, were not exhibited by the homozygote mice (data not shown), and there were no detectable abnormalities in blood cell counts or blood biochemistry (data not shown). Because rescued homozygotes had a shorter life span compared with wild-type controls (Fig. 5*F*),

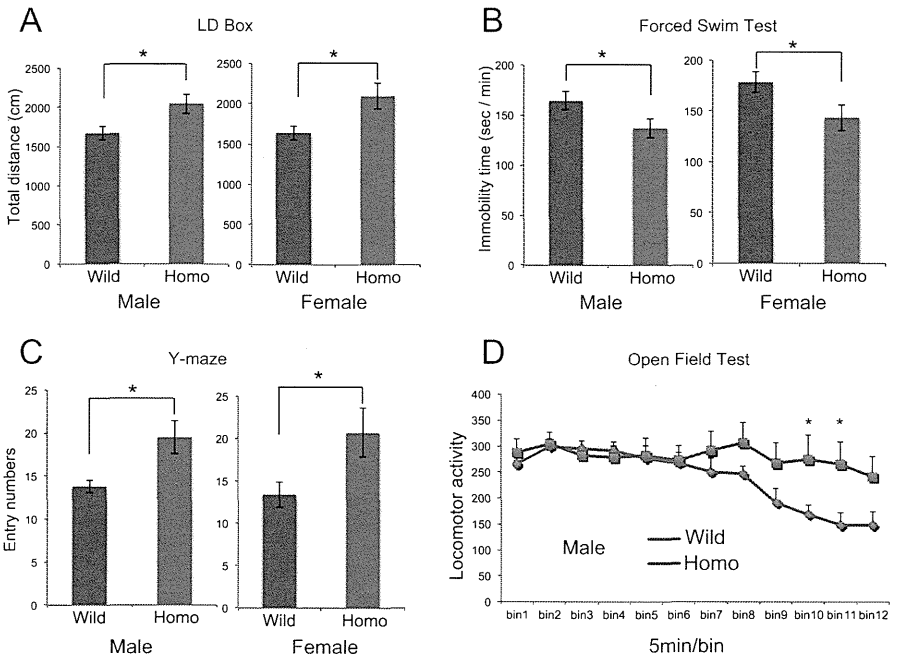

FIGURE 6. **T95K homozygous mutant mice show hyperactivity.** *A–C*, male and female homozygotes were tested in the light-dark (*LD*) box transition (*A*), forced swim (*B*), and Y-maze (*C*) tests. Data are shown as the mean ± S.E. ($n = 10$ for each genotype). *D*, male homozygotes (*Homo*) were tested in the longer version (60 min) of the open field test. Data are shown as the mean ± S.E. ($n = 10$ for each genotype).

we cannot exclude the possibility that the premature deaths were related to side effects of lithium therapy.

DISCUSSION

In this study, using the powerful and robust RGDMS system, we demonstrated in mice that IMPase 1 activity is required for normal development of the mandible and rib cage, as well as normal brain function. Homozygous *Impa1* mutants (Lys-95) rarely survived until weaning, and none survived longer than 7 min after Caesarean delivery at E18.5. It is highly likely that they would still die shortly after birth following a normal gestation period. Of note, *Smit1* (sodium *myo*-inositol transporter 1) KO mice die of congenital central apnea, caused by abnormal respiratory rhythmogenesis (34, 35). Considering the phenotype of *Smit1* KO mice, the lack of IMPase 1 activity in Lys-95 mutants could cause central apnea due to abnormal neuronal development, resulting from reduced intracellular *myo*-inositol concentrations.

We have already reported the spatial expression patterns of *Impa1* and *Impa2* in embryonic stages (E9.5 and E10.5) (21), as well as brain expression during early post-natal stages (P7 and P21) (8). Those results showed *Impa1* is expressed in various areas of the mouse, including the first brachial arch that generates the lower and upper jaws. Although the maxilla (upper jaw) and palate do not appear to be severely affected, the process of mandibular formation is specifically altered in homozygotes. In fact, Meckel's cartilage, an essential structure for mandibular formation, is poorly developed in homozygotes at E14.5 (Fig. 4*B*). In conjunction with the observation that *Smit1* knock-out mice also display a deficiency in osteogenesis (36), these data support a crucial role for free *myo*-inositol in bone formation. Intriguingly, we observed no abnormalities in limb formation (Figs. 3*A* and 4), although the expression of *Impa1* was relatively high in limb buds during embryogenesis (21). A possible explanation could be that expression of inositol transporters such as SMIT and HMIT masks the deleterious effect of *Impa1* deficiency during limb development. Supporting this idea is the observation that *Smit1* knock-out mice have shorter limbs (36). Some genetically engineered mice (*e.g. Dlx5/6*, *Zic2*, *Chd*, and *Nog* KOs) also show abnormal jaw formation (37–39), and some knock-out animals (*Dppa4*, *Ephrin B1*, and *EphB2/EphB3*) exhibit asymmetric fusion of ribs to the sternum (40, 41). Whether and how these morphogenic genes are involved in inositol or inositol phosphate metabolism remain to be determined.

Here, we show that *Impa1* Lys-95 homozygotes were more active in various behavioral tests, compared with their wild-type littermates, demonstrating that IMPase 1 activity is required for normal brain function. In keeping with our results, Cryns *et al.* (42). reported that *Impa1* KO mice are hyperactive in the open field test and exhibit shorter immobility times in the forced swim test compared with control mice. The hyperactivity and altered circadian control seen in our homozygotes were not restored by dietary supplementation with 4% *myo*-inositol during adulthood (Fig. 8, *A–C*). Although the simplest explanation may be that loss of cellular inositol in the adult brain does not precipitate behavioral deficits, we cannot exclude the possibility that *myo*-inositol ingested by these adult animals did not sufficiently penetrate the blood-brain barrier, possibly due to its hydrophilic nature. It should be noted that Cryns *et al.* (42) did not detect a significant reduction in *myo*-inositol content within the brains of adult *Impa1* knock-out mice supplemented with *myo*-inositol, up to the stage of weaning.

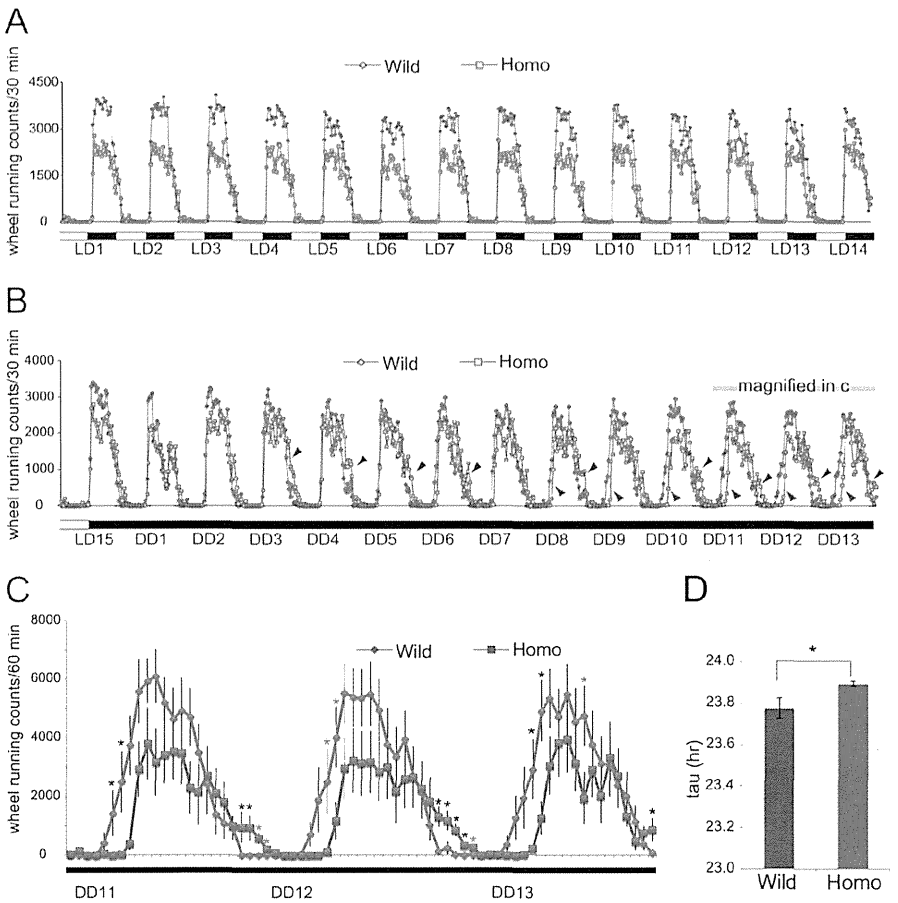

FIGURE 7. **Disturbance of circadian rhythm control in T95K mutants.** *A*, wheel-running activity in 12-h light:12-h dark (*LD*) cycles was monitored for 2 weeks. Data are shown as the mean without *error bars* ($n = 10$ for each genotype). *B*, wheel-running activity in DD cycles was monitored for 13 days. Data are shown as the mean without *error bars*. Homozygotes show delayed activity (*blue* and *red arrowheads*) at later stages of the test. *Red* and *blue arrowheads* indicate delayed onsets and offsets, respectively. *C*, wheel-running activity between DD cycles 11 and 13. Data are shown as the mean ± S.E. ($n = 10$ for each genotype). *Blue asterisks* show significant differences between the two genotypes ($p < 0.05$, post hoc Fisher's PLSD test following two-way repeated analysis of variance). Time points with $p < 0.1$ are indicated by *green asterisks*. *D*, circadian period length of homozygotes. The circadian period (*tau*) is determined. Data are shown as the mean ± S.E. *, $p < 0.05$ (Student's *t* test, $n = 10$ for each genotype).

Lithium salts are a first-line drug therapy for bipolar patients, preventing extreme mood swings. In addition, they are often used to treat refractory depression. When administered to normal mice, lithium promotes antidepressant-like effects in multiple behavioral tests, such as the forced swim and tail suspension tests. As stated earlier, *Impa1* Lys-95 homozygotes and *Impa1* KO mice (42) also exhibit hyper-locomotion. These results support the idea that inhibition of IMPase 1 activity exerts an antidepressant-like effect, similar to that of lithium in rodents and humans. Although mammals express IMPase 2, its activity was only slightly inhibited by lithium in our *in vitro* assay system (8), and *Impa2* KO mice do not exhibit significant behavioral changes (21, 43). Pretreating mice with lithium lowers the threshold for the convulsant effect of pilocarpine, and *Impa1* KO mice show greater sensitivity to pilocarpine (42). The *Impa1* Lys-95 homozygotes, despite low penetrance, develop an epileptic phenotype without pretreatment with pilocarpine and lithium. In totality, these results support the conclusion that IMPase 1 may serve as a molecular target for lithium, in the lithium-pilocarpine model.

Molecular genetics studies suggest pathophysiological associations between mood disorders and circadian dysregulation, including abnormal period and phase of rest-activity rhythms (44–49). This is the first study showing a potential role for the free inositol-producing system in the regulation of activity rhythm. We discovered that shutdown of the IMPase 1 pathway led to a prolonged circadian period. Although lithium is known to lengthen the circadian period in various experimental systems, until now, this effect was thought to be a result of lithium's inhibition of GSK3α/β (50–52). Our results put forward the novel possibility that IMPase inhibition, especially that of IMPase 1, may at least in part, through the effects of lithium, alter the circadian rhythm and thus be related to the efficacy of this drug. Although it is still unknown how inositol depletion mediates its biological consequences, especially on brain function, research groups have set about trying to answer this question. First, Andreassi *et al.* (53) found that *Impa1* mRNA is the most abundant transcript in the axons of rat sympathetic neurons and that axon-specific down-regulation of *Impa1* mRNA induces axon degeneration. Second, IMPase plays an essential

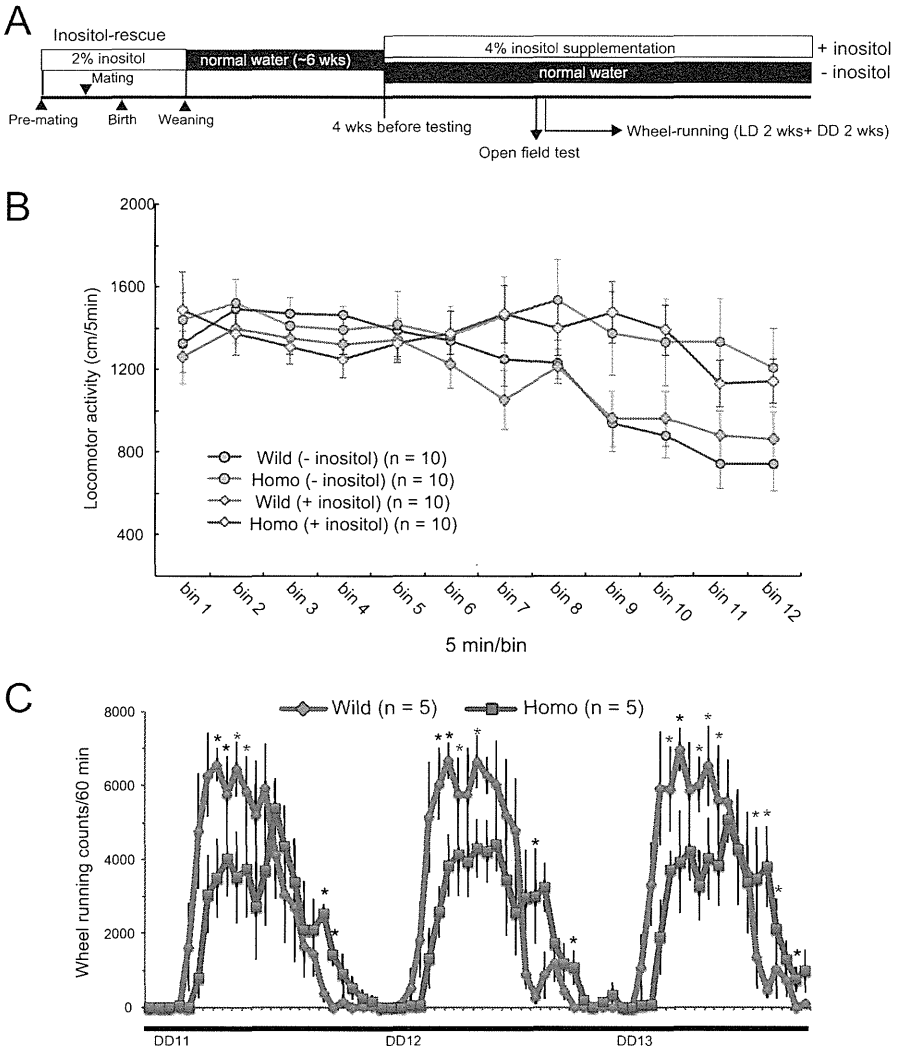

FIGURE 8. **Inositol supplementation does not alleviate behavioral alterations in homozygote mice.** *A*, schematic presentation of experiment schedules. Inositol was supplied for 6 weeks during the weaning period to rescue mutant mice. After this, rescued mice were raised on normal water for 6 weeks and then maintained with or without 4% *myo*-inositol. *B*, open field test. Note that inositol supplementation produced no apparent effect on open field activity in either genotype. *C*, wheel-running activity between DD cycles 11 and 13 under inositol supplementation. Wheel-running activity is presented as in Fig. 7, *C* and *D*.

role in maintaining neuronal polarity as demonstrated by studies on the *Caenorhabditis elegans* gene, *ttx-7*, which is the only nematode gene to encode an IMPase. Mutants of *ttx*-7 are defective in thermotaxis due to disruption of membrane polarity in the RIA neuron (54, 55) and can be rescued by enforced expression of human *IMPA1* or *IMPA2* (21), suggesting that mammalian IMPases and nematode Ttx-7 play similar roles in neurons.

The *Impa1* T95K mutant may therefore serve as a useful tool to dissect the mechanistic action of lithium as a mood stabilizer. Moreover, defining the mechanisms underlying its morphological phenotypes may provide new insights into bone development. Finally, this study illustrates the power of the RGDMS platform to decipher gene function based on the introduction of point mutations, compared with more invasive KO techniques.

Acknowledgments—We thank Drs. Shiroishi, Sakuraba, Uchiyama, Sezutsu, Kaneda, and Furuse for their technical support in identifying mutants. We also thank members of the Research Resources Center of RIKEN BSI for their technical support in DNA sequencing, animal care, blood biochemistry, and cell counting; Y. Ishizuka for animal maintenance, and Dr. Akagi (RRC, RIKEN BSI) and D. Inoue (Materials Characterization Support Unit, RIKEN) for their technical support with electron microscopy observations. We are also grateful to Drs. Abe and Fujisawa for useful discussions.

REFERENCES

1. Berridge, M. J., Downes, C. P., and Hanley, M. R. (1989) Neural and developmental actions of lithium: a unifying hypothesis. *Cell* **59**, 411–419
2. Williams, R. S., Cheng, L., Mudge, A. W., and Harwood, A. J. (2002) A common mechanism of action for three mood-stabilizing drugs. *Nature* **417**, 292–295

3. Harwood, A. J. (2005) Lithium and bipolar mood disorder: The inositol-depletion hypothesis revisited. *Mol. Psychiatry* **10,** 117–126
4. Diehl, R. E., Whiting, P., Potter, J., Gee, N., Ragan, C. I., Linemeyer, D., Schoepfer, R., Bennett, C., and Dixon, R. A. (1990) Cloning and expression of bovine brain inositol monophosphatase. *J. Biol. Chem.* **265,** 5946–5949
5. McAllister, G., Whiting, P., Hammond, E. A., Knowles, M. R., Atack, J. R., Bailey, F. J., Maigetter, R., and Ragan, C. I. (1992) cDNA cloning of human and rat brain myo-inositol monophosphatase. Expression and characterization of the human recombinant enzyme. *Biochem. J.* **284,** 749–754
6. Sjøholt, G., Molven, A., Løvlie, R., Wilcox, A., Sikela, J. M., and Steen, V. M. (1997) Genomic structure and chromosomal localization of a human myo-inositol monophosphatase gene (IMPA). *Genomics* **45,** 113–122
7. Yoshikawa, T., Turner, G., Esterling, L. E., Sanders, A. R., and Detera-Wadleigh, S. D. (1997) A novel human myo-inositol monophosphatase gene, IMP. 18p maps to a susceptibility region for bipolar disorder. *Mol. Psychiatry* **2,** 393–397
8. Ohnishi, T., Ohba, H., Seo, K. C., Im, J., Sato, Y., Iwayama, Y., Furuichi, T., Chung, S. K., and Yoshikawa, T. (2007) Spatial expression patterns and biochemical properties distinguish a second myo-inositol monophosphatase IMPA2 from IMPA1. *J. Biol. Chem.* **282,** 637–646
9. Arai, R., Ito, K., Ohnishi, T., Ohba, H., Akasaka, R., Bessho, Y., Hanawa-Suetsugu, K., Yoshikawa, T., Shirouzu, M., and Yokoyama, S. (2007) Crystal structure of human myo-inositol monophosphatase 2, the product of the putative susceptibility gene for bipolar disorder, schizophrenia, and febrile seizures. *Proteins* **67,** 732–742
10. Fujita, S., Ohnishi, T., Okuda, S., Kobayashi, R., Fukuno, S., Furuta, D., Kikuchi, T., Yoshikawa, T., and Fujita, N. (2011) *In silico* study on the substrate binding manner in human myo-inositol monophosphatase 2. *J. Mol. Model.* **17,** 2559–2567
11. Yoshikawa, T., Kikuchi, M., Saito, K., Watanabe, A., Yamada, K., Shibuya, H., Nankai, M., Kurumaji, A., Hattori, E., Ishiguro, H., Shimizu, H., Okubo, Y., Toru, M., and Detera-Wadleigh, S. D. (2001) Evidence for association of the myo-inositol monophosphatase 2 (IMPA2) gene with schizophrenia in Japanese samples. *Mol. Psychiatry* **6,** 202–210
12. Sjøholt, G., Ebstein, R. P., Lie, R. T., Berle, J. Ø., Mallet, J., Deleuze, J. F., Levinson, D. F., Laurent, C., Mujahed, M., Bannoura, I., Murad, I., Molven, A., and Steen, V. M. (2004) Examination of IMPA1 and IMPA2 genes in manic-depressive patients: association between IMPA2 promoter polymorphisms and bipolar disorder. *Mol. Psychiatry* **9,** 621–629
13. Ohnishi, T., Yamada, K., Ohba, H., Iwayama, Y., Toyota, T., Hattori, E., Inada, T., Kunugi, H., Tatsumi, M., Ozaki, N., Iwata, N., Sakamoto, K., Iijima, Y., Iwata, Y., Tsuchiya, K. J., Sugihara, G., Nanko, S., Osumi, N., Detera-Wadleigh, S. D., Kato, T., and Yoshikawa, T. (2007) A promoter haplotype of the inositol monophosphatase 2 gene (IMPA2) at 18p11.2 confers a possible risk for bipolar disorder by enhancing transcription. *Neuropsychopharmacology* **32,** 1727–1737
14. Nakayama, J., Yamamoto, N., Hamano, K., Iwasaki, N., Ohta, M., Nakahara, S., Matsui, A., Noguchi, E., and Arinami, T. (2004) Linkage and association of febrile seizures to the IMPA2 gene on human chromosome 18. *Neurology* **63,** 1803–1807
15. Gondo, Y., and Fukumura, R. (2009) ENU-induced mutant mice for a next-generation gene-targeting system. *Prog. Brain Res.* **179,** 29–34
16. Gondo, Y., Fukumura, R., Murata, T., and Makino, S. (2009) Next-generation gene targeting in the mouse for functional genomics. *BMB Rep.* **42,** 315–323
17. Gondo, Y., Fukumura, R., Murata, T., and Makino, S. (2010) ENU-based gene-driven mutagenesis in the mouse: A next-generation gene-targeting system. *Exp. Anim.* **59,** 537–548
18. Sakuraba, Y., Sezutsu, H., Takahasi, K. R., Tsuchihashi, K., Ichikawa, R., Fujimoto, N., Kaneko, S., Nakai, Y., Uchiyama, M., Goda, N., Motoi, R., Ikeda, A., Karashima, Y., Inoue, M., Kaneda, H., Masuya, H., Minowa, O., Noguchi, H., Toyoda, A., Sakaki, Y., Wakana, S., Noda, T., Shiroishi, T., and Gondo, Y. (2005) Molecular characterization of ENU mouse mutagenesis and archives. *Biochem. Biophys. Res. Commun.* **336,** 609–616
19. Yamashita, A., Ohnishi, T., Kashima, I., Taya, Y., and Ohno, S. (2001) Human SMG-1, a novel phosphatidylinositol 3-kinase-related protein kinase, associates with components of the mRNA surveillance complex and is involved in the regulation of nonsense-mediated mRNA decay. *Genes Dev.* **15,** 2215–2228
20. McLeod, M. J. (1980) Differential staining of cartilage and bone in whole mouse fetuses by Alcian blue and alizarin red S. *Teratology* **22,** 299–301
21. Ohnishi, T., Tanizawa, Y., Watanabe, A., Nakamura, T., Ohba, H., Hirata, H., Kaneda, C., Iwayama, Y., Arimoto, T., Watanabe, K., Mori, I., and Yoshikawa, T. (2013) Human myo-inositol monophosphatase 2 rescues the nematode thermotaxis mutant ttx-7 more efficiently than IMPA1: Functional and evolutionary considerations of the two mammalian myo-inositol monophosphatase genes. *J. Neurochem.* **124,** 685–694
22. Ohnishi, T., Watanabe, A., Ohba, H., Iwayama, Y., Maekawa, M., and Yoshikawa, T. (2010) Behavioral analyses of transgenic mice harboring bipolar disorder candidate genes, IMPA1 and IMPA2. *Neurosci. Res.* **67,** 86–94
23. Kasahara, T., Kubota, M., Miyauchi, T., Noda, Y., Mouri, A., Nabeshima, T., and Kato, T. (2006) Mice with neuron-specific accumulation of mitochondrial DNA mutations show mood disorder-like phenotypes. *Mol. Psychiatry* **11,** 577–593
24. Singh, N., Halliday, A. C., Knight, M., Lack, N. A., Lowe, E., and Churchill, G. C. (2012) Cloning, expression, purification, crystallization, and x-ray analysis of inositol monophosphatase from *Mus musculus* and *Homo sapiens*. *Acta Crystallogr. Sect. F Struct. Biol. Cryst. Commun.* **68,** 1149–1152
25. Adzhubei, I. A., Schmidt, S., Peshkin, L., Ramensky, V. E., Gerasimova, A., Bork, P., Kondrashov, A. S., and Sunyaev, S. R. (2010) A method and server for predicting damaging missense mutations. *Nat. Methods* **7,** 248–249
26. Arguello, P. A., and Gogos, J. A. (2006) Modeling madness in mice: One piece at a time. *Neuron* **52,** 179–196
27. Baker, M. (2011) Animal models: inside the minds of mice and men. *Nature* **475,** 123–128
28. Beaulieu, J. M., Zhang, X., Rodriguiz, R. M., Sotnikova, T. D., Cools, M. J., Wetsel, W. C., Gainetdinov, R. R., and Caron, M. G. (2008) Role of GSK3β in behavioral abnormalities induced by serotonin deficiency. *Proc. Natl. Acad. Sci. U.S.A.* **105,** 1333–1338
29. Clapcote, S. J., Lipina, T. V., Millar, J. K., Mackie, S., Christie, S., Ogawa, F., Lerch, J. P., Trimble, K., Uchiyama, M., Sakuraba, Y., Kaneda, H., Shiroishi, T., Houslay, M. D., Henkelman, R. M., Sled, J. G., Gondo, Y., Porteous, D. J., and Roder, J. C. (2007) Behavioral phenotypes of Disc1 missense mutations in mice. *Neuron* **54,** 387–402
30. Del Pino, I., García-Frigola, C., Dehorter, N., Brotons-Mas, J. R., Alvarez-Salvado, E., Martínez de Lagrán, M., Ciceri, G., Gabaldón, M. V., Moratal, D., Dierssen, M., Canals, S., Marín, O., and Rico, B. (2013) Erbb4 deletion from fast-spiking interneurons causes schizophrenia-like phenotypes. *Neuron* **79,** 1152–1168
31. Powell, C. M., and Miyakawa, T. (2006) Schizophrenia-relevant behavioral testing in rodent models: A uniquely human disorder? *Biol. Psychiatry* **59,** 1198–1207
32. McClung, C. A. (2011) Circadian rhythms and mood regulation: insights from pre-clinical models. *Eur. Neuropsychopharmacol.* **21,** S683–S693
33. McClung, C. A. (2013) How might circadian rhythms control mood? Let me count the ways. *Biol. Psychiatry* **74,** 242–249
34. Berry, G. T., Wu, S., Buccafusca, R., Ren, J., Gonzales, L. W., Ballard, P. L., Golden, J. A., Stevens, M. J., and Greer, J. J. (2003) Loss of murine Na^+/myo-inositol cotransporter leads to brain myo-inositol depletion and central apnea. *J. Biol. Chem.* **278,** 18297–18302
35. Chau, J. F., Lee, M. K., Law, J. W., Chung, S. K., and Chung, S. S. (2005) Sodium/myo-inositol cotransporter-1 is essential for the development and function of the peripheral nerves. *FASEB J.* **19,** 1887–1889
36. Dai, Z., Chung, S. K., Miao, D., Lau, K. S., Chan, A. W., and Kung, A. W. (2011) Sodium/myo-inositol cotransporter 1 and myo-inositol are essential for osteogenesis and bone formation. *J. Bone Miner. Res.* **26,** 582–590
37. Inoue, T., Hatayama, M., Tohmonda, T., Itohara, S., Aruga, J., and Mikoshiba, K. (2004) Mouse Zic5 deficiency results in neural tube defects and hypoplasia of cephalic neural crest derivatives. *Dev. Biol.* **270,** 146–162
38. Stottmann, R. W., Anderson, R. M., and Klingensmith, J. (2001) The BMP antagonists Chordin and Noggin have essential but redundant roles in mouse mandibular outgrowth. *Dev. Biol.* **240,** 457–473
39. Depew, M. J., Lufkin, T., and Rubenstein, J. L. (2002) Specification of jaw subdivisions by Dlx genes. *Science* **298,** 381–385

40. Madan, B., Madan, V., Weber, O., Tropel, P., Blum, C., Kieffer, E., Viville, S., and Fehling, H. J. (2009) The pluripotency-associated gene Dppa4 is dispensable for embryonic stem cell identity and germ cell development but essential for embryogenesis. *Mol. Cell. Biol.* **29,** 3186–3203
41. Compagni, A., Logan, M., Klein, R., and Adams, R. H. (2003) Control of skeletal patterning by ephrinB1-EphB interactions. *Dev. Cell* **5,** 217–230
42. Cryns, K., Shamir, A., Van Acker, N., Levi, I., Daneels, G., Goris, I., Bouwknecht, J. A., Andries, L., Kass, S., Agam, G., Belmaker, H., Bersudsky, Y., Steckler, T., and Moechars, D. (2008) IMPA1 is essential for embryonic development and lithium-like pilocarpine sensitivity. *Neuropsychopharmacology* **33,** 674–684
43. Cryns, K., Shamir, A., Shapiro, J., Daneels, G., Goris, I., Van Craenendonck, H., Straetemans, R., Belmaker, R. H., Agam, G., Moechars, D., and Steckler, T. (2007) Lack of lithium-like behavioral and molecular effects in IMPA2 knockout mice. *Neuropsychopharmacology* **32,** 881–891
44. Artioli, P., Lorenzi, C., Pirovano, A., Serretti, A., Benedetti, F., Catalano, M., and Smeraldi, E. (2007) How do genes exert their role? Period 3 gene variants and possible influences on mood disorder phenotypes. *Eur. Neuropsychopharmacol.* **17,** 587–594
45. Lamont, E. W., Legault-Coutu, D., Cermakian, N., and Boivin, D. B. (2007) The role of circadian clock genes in mental disorders. *Dialogues Clin. Neurosci.* **9,** 333–342
46. McClung, C. A. (2007) Circadian genes, rhythms and the biology of mood disorders. *Pharmacol. Ther.* **114,** 222–232
47. Barnard, A. R., and Nolan, P. M. (2008) When clocks go bad: neurobehavioural consequences of disrupted circadian timing. *PLoS Genet.* **4,** e1000040
48. Kripke, D. F., Nievergelt, C. M., Joo, E., Shekhtman, T., and Kelsoe, J. R. (2009) Circadian polymorphisms associated with affective disorders. *J. Circadian Rhythms* **7,** 2
49. Mendlewicz, J. (2009) Disruption of the circadian timing systems: Molecular mechanisms in mood disorders. *CNS Drugs* **23,** 15–26
50. Dokucu, M. E., Yu, L., and Taghert, P. H. (2005) Lithium- and valproate-induced alterations in circadian locomotor behavior in *Drosophila*. *Neuropsychopharmacology* **30,** 2216–2224
51. Lavoie, J., Hébert, M., and Beaulieu, J. M. (2013) Glycogen synthase kinase-3β haploinsufficiency lengthens the circadian locomotor activity period in mice. *Behav. Brain Res.* **253,** 262–265
52. Yin, L., Wang, J., Klein, P. S., and Lazar, M. A. (2006) Nuclear receptor Rev-erbα is a critical lithium-sensitive component of the circadian clock. *Science* **311,** 1002–1005
53. Andreassi, C., Zimmermann, C., Mitter, R., Fusco, S., De Vita, S., Devita, S., Saiardi, A., and Riccio, A. (2010) An NGF-responsive element targets myo-inositol monophosphatase-1 mRNA to sympathetic neuron axons. *Nat. Neurosci.* **13,** 291–301
54. Kimata, T., Tanizawa, Y., Can, Y., Ikeda, S., Kuhara, A., and Mori, I. (2012) Synaptic polarity depends on phosphatidylinositol signaling regulated by myo-inositol monophosphatase in *Caenorhabditis elegans*. *Genetics* **191,** 509–521
55. Tanizawa, Y., Kuhara, A., Inada, H., Kodama, E., Mizuno, T., and Mori, I. (2006) Inositol monophosphatase regulates localization of synaptic components and behavior in the mature nervous system of *C. elegans*. *Genes Dev.* **20,** 3296–3310

PLOS ONE

Sleep Debt Elicits Negative Emotional Reaction through Diminished Amygdala-Anterior Cingulate Functional Connectivity

Yuki Motomura[1,2], Shingo Kitamura[1], Kentaro Oba[1], Yuri Terasawa[1], Minori Enomoto[1], Yasuko Katayose[1], Akiko Hida[1], Yoshiya Moriguchi[1], Shigekazu Higuchi[3], Kazuo Mishima[1]*

1 Department of Psychophysiology, National Institute of Mental Health, National Center of Neurology and Psychiatry, 4-1-1 Ogawa-Higashi, Kodaira, Tokyo, Japan, **2** Graduate School of Integrated Frontier Science, Kyushu University 6-10-1 Hakozaki, Higashi-ku, Fukuoka, Japan, **3** Faculty of Design, Kyushu University 4-9-1 Shiobaru, Minami-ku, Fukuoka, Japan

Abstract

Objectives: Sleep debt reportedly increases emotional instability, such as anxiety and confusion, in addition to sleepiness and psychomotor impairment. However, the neural basis of emotional instability due to sleep debt has yet to be elucidated. This study investigated changes in emotional responses that are elicited by the simulation of short-term sleep loss and the brain regions responsible for these changes.

Subjects and Methods: Fourteen healthy adult men aged 24.1±3.3 years (range, 20–32 years) participated in a within-subject crossover study consisting of 5-day sessions of both sleep debt (4 h for time in bed) and sleep control (8 h for time in bed). On the last day of each session, participants underwent polysomnography and completed the State-Trait Anxiety Inventory and Profile of Mood States questionnaires. In addition, functional magnetic resonance imaging was conducted while performing an emotional face viewing task.

Results: Restricted sleep over the 5-day period increased the activity of the left amygdala in response to the facial expression of fear, whereas a happy facial expression did not change the activity. Restricted sleep also resulted in a significant decrease in the functional connectivity between the amygdala and the ventral anterior cingulate cortex (vACC) in proportion to the degree of sleep debt (as indicated by the percentage of slow wave sleep and δ wave power). This decrease was significantly correlated with activation of the left amygdala and deterioration of subjective mood state.

Conclusion: The results of this study suggest that continuous and accumulating sleep debt that can be experienced in everyday life can downregulate the functional suppression of the amygdala by the vACC and consequently enhance the response of the amygdala to negative emotional stimuli. Such functional alteration in emotional control may, in part, be attributed to the neural basis of emotional instability during sleep debt.

Citation: Motomura Y, Kitamura S, Oba K, Terasawa Y, Enomoto M, et al. (2013) Sleep Debt Elicits Negative Emotional Reaction through Diminished Amygdala-Anterior Cingulate Functional Connectivity. PLoS ONE 8(2): e56578. doi:10.1371/journal.pone.0056578

Editor: Namni Goel, University of Pennsylvania School of Medicine, United States of America

Received September 5, 2012; **Accepted** January 12, 2013; **Published** February 13, 2013

Funding: This study was supported in part by a Grant-in-Aid for the Strategic Research Program for Brain Sciences (Understanding of molecular and environmental bases for brain health) from the Ministry of Education, Culture, Sports, Science and Technology of Japan (URL: http://brainprogram.mext.go.jp/), an Intramural Research Grant (23-3) for Neurological and Psychiatric Disorders from NCNP(URL:http://www.ncnp.go.jp/), and KAKENHI (21390335)(URL:http://www.jsps.go.jp/j-grantsinaid/). The funders had no role in study design, data collection and analysis, decision to publish, or preparation of the manuscript.

Competing Interests: The authors have declared that no competing interests exist.

* E-mail: mishima@ncnp.go.jp

Introduction

Many people are now suffering from chronic sleep loss as a result of today's 24-h society, night-owl lifestyles, and prolonged work hours becoming a normal state of everyday life [1,2,3,4,5,6]. Sleep loss causes day-time sleepiness and psychomotor impairment, and can result in human errors and accidents [7,8,9].

Acute sleep deprivation has been shown to augment physiological and psychological reactions to emotional stimuli. For example, compared with normal sleep conditions, overnight total sleep deprivation enhances sympathetic reactions to unpleasant stimuli, such as dilation of the pupils and increased heart rate and blood pressure [10,11], declined task performance due to increased interference of working memory by unpleasant emotional stimuli [12], and increased changes in mood deterioration triggered even by weak emotional stressors [13]. According to functional brain imaging studies investigating the neural basis of emotional responses after acute sleep deprivation, unpleasant emotional stimuli increase the activity of the amygdala after overnight total sleep deprivation, suggesting a decline in functional connectivity between the amygdala and the medial prefrontal cortex (mPFC) which may reflect decreased inhibition by the frontal lobe [12,14].

In addition, Swann et al. have shown that response time to subliminal priming is shortened after having short hours of sleep over a 2-day period [15]. Because subliminal visual information is transmitted to the amygdala without going through the visual

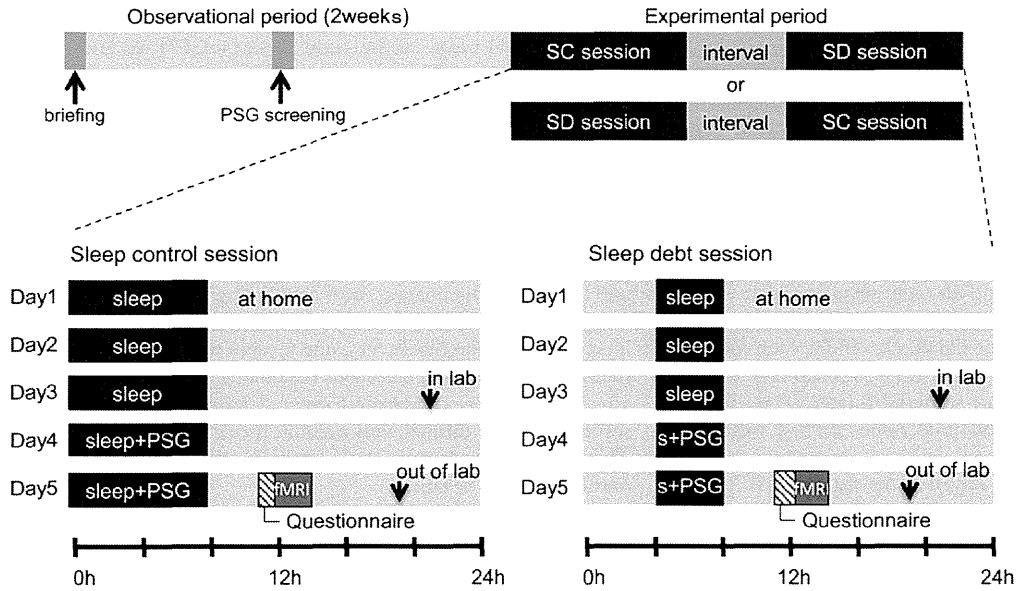

Figure 1. Experimental protocol. The study was conducted in a randomized crossover design, involving a sleep control (SC) and sleep debt (SD) session (for 5 days in each session) with a 2-week interval between the sessions. In the observational session before the experiment, participants visited the laboratory for a briefing session and gave their informed consent. One week later, participants came to the lab for PSG screening. One week after the PSG screening, the experimental sessions were started, with the order of the sessions counter-balanced across participants (i.e., SC-SD or SD-SC). Participants stayed at home on days 1–3 within each SC and SD session, according to the restrictive sleep-wake schedule that had been already instructed in the briefing (i.e., sleep time of 8 h for SC and 4 h for SD). Participants came to the lab on night 3 of the SC and SC sessions and spent the rest of the sessions (i.e., 2 days per session) in the sleep-lab with their sleep time controlled as instructed. On nights 3 and 4 in each session, participants underwent PSG measurement in the lab. On day 5, they completed questionnaires to check their mood state and sleepiness followed by fMRI scanning with an emotional task. SC, sleep control; SD, sleep debt; PSG, polysomnography; SSS, Stanford Sleepiness Scale; STAI, State-Trait Anxiety Inventory; POMS, Profile of Mood States.
doi:10.1371/journal.pone.0056578.g001

cortex [16,17,18,19,20] and subliminal and supraliminal stimulation induce different responses in the amygdala [21,22], it is possible that the transduction through subliminal signal pathways may also play an important role in changes in emotional responses to visual stimuli after sleep deprivation.

On the other hand, deteriorated mental and physical conditions due to sleep loss (partial sleep deprivation) are more likely to be caused by an accumulation of short sleep episodes over several days (sleep debt) than overnight total sleep deprivation [23]. Although sleep debt reportedly augments emotional instability (including anxiety and confusion), together with sleepiness, the feeling of fatigue, and deficits in psychomotor performance [24,25,26,27,28], the characteristics of emotional responses induced by sleep debt and the neural basis underlying such responses have not been studied extensively and therefore remain unclear.

In this study, we simulated continuous and accumulating sleep debt that can be experienced in everyday life (short hours of sleep over a 5-day period) to investigate changes in emotional responses caused by visual stimuli presented above and below the level of consciousness and the brain regions responsible for these changes.

Materials and Methods

Ethics Statement

This study was approved by the Ethics Committee of the National Center of Neurology and Psychiatry, Japan and was conducted in accordance with the Declaration of Helsinki.

Participants

This study involved 14 healthy, right-handed adult men (mean ± SD age, 24.1±3.32 years) who provided written informed consent to participate. All participants were Japanese and native Japanese speakers. A sleep log and actigraph (Ambulatory Monitoring Inc., Ardsley, NY) were used to monitor the sleep schedule of participants during the observational period (a 2-week period prior to the study) and the following experimental period. Using Cole's algorithm with optimal parameters [29], sleep-onset time, wake time, and the amount of time awake in bed were calculated from the actigraph data and were compared with the sleep log to confirm the absence of irregular life patterns, such as working in shifts or staying up all night. Overnight polysomnography (PSG) was also conducted during the observational period to examine for sleep disorders.

Exclusion criteria were as follows: a mean bedtime or wakeup time during the observational period outside of the hours 23:00–02:00 and 07:00–10:00, respectively(including shift worker); some form of sleep disorder; serious physical complication; psychiatric disorder; ocular disease, including achromatopsia; taking medication or substances inveterately that might affect the experimental data (e.g., steroids and drugs that induce drowsiness such as hypnotics and anti-histamines); caffeine intake of over 200 mg per day, heavy smoker (stressed by a 5-day smoking cessation) implanted metal object such as a pacemaker; working shifts (engaged in shift work in the 4 weeks preceding the study); or travelling to a country with a 6-h time difference in the 3 months preceding the study.

Sleep restriction protocol

Figure 1 shows the experimental protocol. All participants attended the briefing session concerning the experimental outline, underwent sleep electroencephalography (EEG) screening during the 2-week observational period, and participated in two 5-day experimental sessions. The number of hours in bed (i.e., after lights-out and during sleep) was 8 h/day in the sleep control (SC) session and 4 h in the sleep debt (SD) session. Both sessions were conducted as a crossover study with a 2-week interval between the sessions. During the interval, participants were asked to maintain a regular lifestyle without staying up all night or taking shift work.

In the SC session, based on the sleep log and actigram from the observation period, mean bedtime (23:00–02:00) for each individual was used as the start time for 8 h of sleep (wakeup time 07:00–10:00). In the SD session, bedtime started 4 h later (03:00–06:00) than that in the SC session and total hours in bed were 4 h (wakeup time 07:00–10:00).

In both sessions, participants stayed home for the first 3 days and then stayed in a laboratory room at the National Center of Neurology and Psychiatry for the next 2 days. To maintain the strict wakeup time at home, we sent a mail alert every 4 h, starting at the scheduled wakeup time until bedtime, and asked participants to answer the mail immediately. Participants were instructed by E-mail to refrain from caffeine and alcohol intake and smoking during the 5 days in which the sessions were held. In the laboratory, participants were under video camera surveillance, always assisted by a research attendant, and verbally awakened when in a drowsy state, such taking a nap or dozing off. During the wake period, participants were allowed to move freely around the laboratory, read and write, enjoy music and videos, play videogames, and engage in conversation with a researcher. Mineral water was always available, but the intake of caffeine and alcohol, smoking, and heavy exercise were restricted. Ambient temperature and humidity in the laboratory were maintained at 25±0.5°C and 50±5% RH, respectively.

MRI and emotional face viewing task

Magnetic resonance imaging (MRI) was performed on day 5 of the sessions. Participants were first served the same breakfast (~350-kcal sandwich) within 2 h of wakeup time before entering a room next to the MRI room 2–2.5 h after the wakeup time to answer a questionnaire about subjective sleepiness and mood. They underwent MRI 3–5 h after wakeup time.

During MRI, participants viewed faces with emotional expressions under two different conditions: (1) the conscious condition with a sufficient viewing time to allow supraliminal visual perception of an emotional facial expression and (2) the non-conscious condition with a brief viewing time to perform subliminal perception of an emotional facial expression followed by a neutral facial expression to mask the emotional facial image (Fig. 2).

We selected portraits of 16 individuals (4 Caucasian men, 4 Caucasian women, 4 Japanese men, and 4 Japanese women) from two standardized image sets ([30,31]www.atr-p.com/face-db.html) and created 3 facial images per individual representing the categories of fear, happy, and neutral facial expressions by masking the hair and background (48 images in total).

(1) Under the conscious condition, a fixation image was presented for 1000 ms, followed by one of the three types of facial expressions for 200 ms and then a blank image for 1000 ms. (2) Under the non-conscious condition, after presenting a fixation image for 1000 ms, either (i) a neutral facial image was presented for 26 ms, followed by a neutral facial image of another person of the same sex for 174 ms and then a blank image for 1000 ms, or (ii) a happy (fear) facial image was presented for 26 ms, followed by a neutral facial image of the same person for 174 ms and then a blank image for 1000 ms.

In both the conscious and non-conscious presentations, therefore, one trial consisted of the presentations of a fixation image, a facial image in the conscious condition or two images in the non-conscious condition, and a blank image. Nine trials composed one block. Among each block of 9 trials, a target stimulus was presented randomly, to which participants were to respond by pressing a button in order to keep themselves awake and focused on the images. After completing each block, a fixation image was shown on the screen for 15 s (baseline). A total of 12 image presentation blocks (i.e., one session) were conducted under the non-conscious and conscious conditions (6 blocks each) with a 15-s baseline period provided every 2 blocks, and a total of 2 sessions were performed with a 2-min break between the sessions. The order of block presentation was counter-balanced between participants and sessions.

Questionnaire

The Stanford Sleepiness Scale (SSS; [32]) was used to assess subjective sleepiness. Subjective mood was evaluated using state components of the State-Trait Anxiety Inventory (STAI-S; [33]), as well as the Profile of Mood States (POMS; [34]). During the SC and SD sessions, participants answered the questionnaire immediately prior to MRI.

Polysomnography (PSG) and delta wave power analysis

On nights 4 and 5 of each session, PSG was performed and analyzed using the Neurofax EEG-1200 (Nihon Kohden Corporation, Tokyo, Japan) with Ag/AgCl electrodes. The system recorded an electrocardiogram (ECG), electrooculogram (EOG), electromyogram of the chin (Chin-EMG), and electroencephalogram (EEG) at C3, C4, O1, and O2 sites in line with the International 10–20 system using the mastoid processes as reference points. The sampling rate was 200 Hz, and the hardware bandpass filter was set at 0.5–35 Hz. EEG recordings from C3-A2 were used to perform visual classification of sleep stages in 30-s epochs in accordance with international sleep scoring parameters [35].

The PSG data obtained on night 4 was excluded from the analysis to eliminate the first night effect [36]. The following sleep parameters were calculated from the PSG data taken on night 5: total sleep time (TST), duration of each sleep stage, duration of slow wave sleep (Stage 3+4; SWS) during the 2-h period after bedtime, sleep latency (SL), sleep efficiency (SE), percentage of SWS spent in TST (%SWS), and percentage of rapid eye movement (REM) sleep (%REM).

Because sleep debt increases the duration of SWS and delta power during the initial stage of sleep [27,37,38,39,40], during the first 2 h after bedtime the amounts of SWS ($SWS_{2\ h}$) and δ power ($\delta_{2\ h}$, 0.5–4 Hz) were used as objective indicators of sleep debt.

After visually excluding epochs containing body movement artifacts, all NREM sleep epochs (Stages 2–4) in the C3 EEG recording were analyzed using the fast Fourier transform (5.12-s hamming window, 2.5-s steps), and based on the power values obtained every 0.2 Hz, δ power (0.5–4 Hz) was calculated.

fMRI acquisition

The Siemens Magnetom Verio 3T MRI system was used in the analysis. To obtain reference images for analysis, structural images (T1-weighted magnetization-prepared rapid gradient-echo (MPRAGE) images) were taken with the following sequence

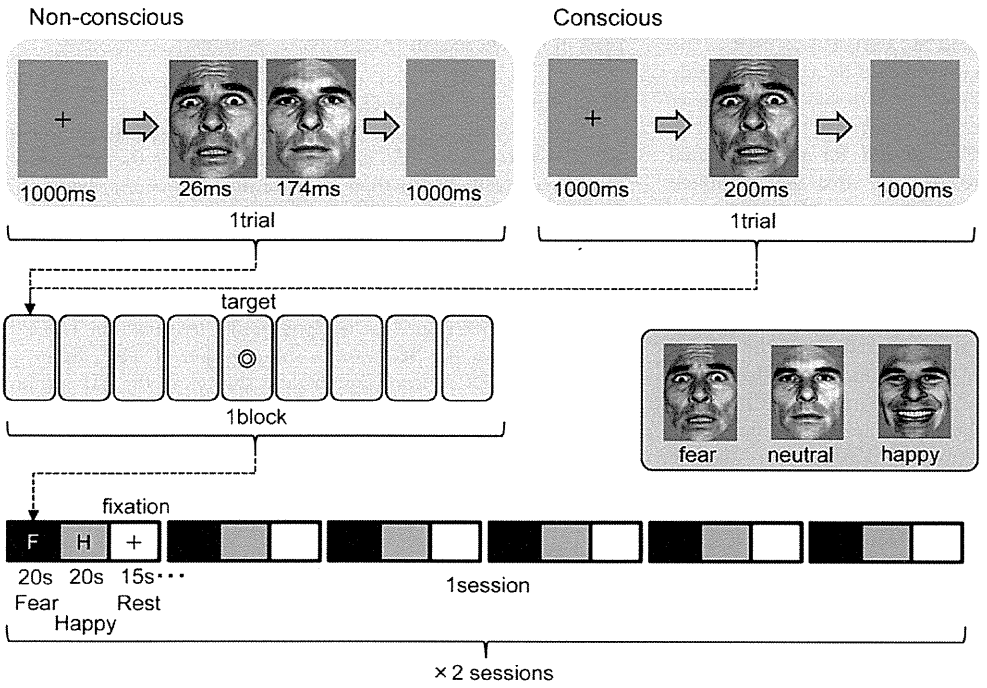

Figure 2. Design of emotional facial presentations. Facial pictures depicting fear or happy (i.e., emotional) or neutral expressions were used as the stimuli and were presented either non-consciously or consciously. In a non-conscious trial, an emotional image (either fear, happy, or neutral) was implicitly presented for 26 ms, followed by an explicit presentation for 174 ms of a neutral 'masking' face of the same identity as the preceding implicit emotional face (when the implicit face was neutral, the following explicit mask was of a different person of the same sex). Participants were required to press a button in response to each 'target' stimulus to keep themselves awake during the scanning.
doi:10.1371/journal.pone.0056578.g002

parameters: TR/TE = 1900/2.52 ms, voxel size = 1×1×1 mm, flip angle 9°, and field of view = 256×192 mm.

A single shot echo-planar imaging technique was used to obtain task-related functional MRI (fMRI) images. Settings were: TR/TE = 2500/25 ms, 30 axial slices, voxel size = 3×3×4 mm, 1-mm inter slice gap, flip angle 90°, matrix size = 64×64, and field of view = 192×192 mm. Of 137 scanning images obtained in each session, the first 5 images were excluded from analysis.

fMRI data analysis

SPM8 (Wellcome Department of Imaging Neuroscience, http://www.fil.ion.ucl.ac.uk/spm/software/spm8/) was used in the analysis of functional brain imaging data. For each image, motion and slice timing correction as well as co-registration into an MPRAGE structural image was performed. MPRAGE imaging was carried out after PSG screening. The Montreal Neurological Institute (MNI) template was used for spatial normalization, and smoothing was performed using an 8-mm full width of half maximum Gaussian kernel. MRI time-series data that contained the three-dimensional blood oxygenation level dependent (BOLD) signals of each participant were analyzed using the first-level fixed effect model with general linear model (GLM) regression analysis. Using the canonical hemodynamic response model implemented in SPM8, a hypothetical hemodynamic time course corresponding to the stimulus presentations under each task condition was developed by convolving the canonical function. Thirteen hemodynamic models of time series corresponding to i) 6 conditions [3 categories of emotions (happy, fear, and neutral)×2 types of image presentation (conscious/non-conscious)], ii) target image presentation, and iii) 6 head motions as regressors were incorporated into the design matrix. Actual BOLD signals were analyzed voxel by voxel using the GLM, and the parameter estimate for each regressor was calculated. To subtract the low visual features, contrasts were created by subtracting the activity at the time of neutral facial image presentation from the activity at the time of emotional facial image presentation. Consequently, a total of 4 contrasts for a fear vs. neutral facial image and happy vs. neutral facial image under the conscious and non-conscious conditions were created.

To determine differences between the SC and SD sleep conditions, the value of the first-level contrast images in each SC and SD session were entered into a paired *t*-test implemented in SPM, with SC/SD as a within-subject factor.

Based on the hypothesis that sleep debt enhances the activity of the amygdala [14], we set the amygdala as the region of interest (ROI) and searched for the area where the activation was higher during the SD session than the SC session. Using the PickAtlas software (Wake Forest University (WFU), http://fmri.wfubmc.edu/downloads/WFU_PickAtlas_User_Manual.pdf) in the SPM Toolbox, masks for the amygdala on both sides were generated based on Anatomical Automatic Labeling (AAL), and each voxel in the mask was analyzed. Data were considered significant if p was less than 0.001 and the number of continuous voxels forming a cluster was greater than 5 within the amygdala ROIs. Furthermore, the significant cluster was corrected by family-wise error (FWE) correction within the amygdala ROIs ($p<0.05$, small volume correction [41]).

Functional connectivity analysis

To reveal the functional connectivity related to enhanced amygdala activation during sleep debt, a cluster in the left amygdala (peak MNI coordinates x = −14, y = 4, z = −18, 8

voxels, see Results) that exhibited a significant difference in fear vs. neutral contrast between the SD and SC sessions was used as the seed region of the connectivity analysis. Based on a previous study hypothesizing that sleep debt weakens the functional connectivity between the amygdala and the mPFC adjacent to the ACC [14], we placed the ROI in the mPFC region for the functional connectivity analysis and searched for the area that exhibited greater connectivity with the seed region in the SC session than that in the SD session. Using the WFU PickAtlas software in the SPM Toolbox, a mask for the ACC/mPFC region was generated based on AAL (by combining 'anterior cingulate' and 'medial frontal gyrus'), and each voxel in the mask was analyzed. The functional connectivity between the amygdala and the ACC/mPFC was analyzed using the CONN tool (Alfonso Nieto-Castanon, http://www.alfnie.com/software/conn) of SPM8.

Using GLM, voxels that were activated in relation to the BOLD signals in the seed region were extracted. Head motions and the hypothetical hemodynamic response to the main event (confounding effects of stimulus-locked transients [42]) and to the target were used as regressors, and the range of the bandpass-filter was set at 0.008–0.09 Hz. Connectivity contrasts thus created were used in first-level and second-level analyses, as in the analysis described earlier in the 'fMRI data analysis' section. Data were considered significant if p was less than 0.001 and the number of continuous voxels forming a cluster was greater than 5. Because of the larger size of the mask in the MPFC/ACC region, the small volume correction was not performed in functional connectivity analysis.

Correlation analysis between mood/sleep changes and fMRI data

Differences in the values between sessions were calculated for subjective mood (scores from the STAI-S and POMS questionnaires), $SWS_{2\ h}$, and $\delta_{2\ h}$. The contrast values between the sessions were also calculated for 1) amygdala activation and 2) the intensity of functional connectivity between the left amygdala and the ventral anterior cingulate cortex ($FC_{amg\text{-}vACC}$) in the fear vs. neutral condition under conscious presentation. Correlations between these psychometric and imaging contrast values were analyzed.

Clusters used in the analysis were the left amygdala, which showed differential activation between the SD and SC sessions, and the vACC, which showed different degrees of functional connectivity with the amygdala, as the seed region, between the sessions. Marsbar software (Matthew Brett, http://marsbar.sourceforge.net/marsbar.pdf) was used to calculate the mean contrast values in a cluster.

Statistics

The SPSS PASW Statistics 18 software package was used in statistical analysis. Differences in questionnaire scores, PSG data, and values of δ power between the SD and SC sessions were analyzed using the two-tailed t-test. Results are expressed as mean ± SD. Between-subjects test was performed by calculating Pearson's product moment correlation coefficient. Except for the analysis of functional brain activity, data were considered significant at $p<0.05$.

Results

Sleep time regulation

From the actigraph data, mean sleep time over the entire 5-day period in the SC and SD sessions was 8.09±0.35 h (8 h 5 min±21 min) and 4.60±0.54 h (4 h 36 min±32 min), with significantly fewer sleep hours (3.48±0.54 h, or 3 h 29 min±32 min) in the SD session [$t(13) = 24.17$, $p<0.001$].

Sleepiness and mood states

Table 1 shows sleepiness and mood states associated with the SC and SD sessions. SSS and STAI-S scores for the SD session were significantly higher than those for the SC session, whereas no significant session-related differences were seen in POMS subscale scores.

PSG/delta wave power data

Sleep parameters and the analysis results are shown in Table 2. Compared with the SC session, the duration of TST, Stage 1, Stage 2, and REM were significantly shorter in the SD session; however, no differences were observed with Stage 3+4 or $SWS_{2\ h}$. As a result, the SD session had significantly higher %SWS and SE and significantly shorter SL. In addition, $\delta_{2\ h}$ for the SD session was significantly higher than that for the SC session.

Button Response

No significant session-related differences were seen in either the number or the mean time of responses (SC = 11.63±0.6, SD = 11.38±1.16, SC = 596.98±0.153.43, SD = 608.28±115.34, respectively).

fMRI activation

Comparison of fear vs. neutral contrasts for the conscious condition revealed significantly greater activation of the left amygdala in the SD session than in the SC session [peak MNI coordinates x = −14, y = 4, z = −18, $t(13) = -5.60$, FWE $p<0.05$ small volume correction] (Fig. 3; Table 3). Even though the activation of the right amygdala in the SD session was also higher than that in the SC session, it did not reach the significance level set for the analysis[peak MNI coordinates x = 18, y = 2, z = −18, $t(13) = -3.41$, $p = 0.002$]. With regard to happy vs. neutral contrasts, the amygdala showed no session-related differences in activation [left amygdala, x = −14, y = 4, z = −14, $t(13) = -3.04$; right amygdala, x = 16, y = 2, z = −16, $t(13) = -1.90$].

Under the non-conscious condition, no significant differences in amygdala activation between the sessions was observed with fear vs. neutral contrasts [left amygdala; x = −14, y = −8, z = −16,

Table 1. Subjective sleepiness and mood state scores for the sleep control (SC) and sleep debt (SD) sessions; t and p-values for SC vs. SD with the paired t-test.

	SC session	SD session	t	p
SSS	2.14 (0.66)	3.21 (1.05)	−3.51	<0.01
STAI-state	35.64 (6.21)	39.43 (4.86)	−2.74	<0.05
POMS Vigor	53.54 (10.02)	53.54 (11.57)	0.00	N.S.
POMS Depression	47.76 (9.00)	48.13 (8.71)	−0.40	N.S.
POMS Anger-Hostility	42.84 (4.52)	42.24 (6.18)	0.60	N.S.
POMS Fatigue	45.94 (6.61)	48.13 (7.48)	−1.30	N.S.
POMS Tension-Anxiety	46.37 (10.57)	47.05 (9.92)	−0.46	N.S.
POMS Confusion	48.12 (8.07)	49.94 (9.32)	−0.99	N.S.

Data are expressed as mean (standard deviation) values; SSS, Stanford Sleepiness Scale; STAI, State-Trait Anxiety Inventory.
POMS, Profile of Mood States.
Degrees of freedom (df) = 13.
doi:10.1371/journal.pone.0056578.t001

Table 2. Values of spectral analysis and sleep variables for the sleep control (SC) and sleep debt (SD) sessions; *t* and *p*-values for SC vs. SD with the paired *t*-test.

	SC session	SD session	*t*	*p*
TST (min)	446.7 (22.5)	233.5 (7.5)	38.71	<0.001
Stage1 (min)	35.8 (20.0)	10.8 (8.2)	5.31	<0.001
Stage2 (min)	236.9 (35.3)	107.3 (28.9)	15.25	<0.001
Stage3 (min)	40.0 (11.3)	39.6 (15.4)	0.13	N.S.
Stage4 (min)	20.9 (25.8)	24.1 (25.8)	−1.52	N.S.
SWS (min)	60.8 (28.7)	63.7 (26.7)	−0.70	N.S.
REM (min)	113.1 (21.2)	51.7 (17.1)	11.09	<0.001
$SWS_{2\ h}$ (min)	37.5 (18.6)	41.4 (18.4)	−1.27	N.S.
Sleep latency (min)	19.3 (23.5)	3.3 (4.9)	2.90	<0.05
%SWS (%)	13.7 (6.7)	27.3 (11.6)	−7.21	<0.001
%REM (%)	25.4 (4.7)	22.2 (7.2)	1.80	N.S.
Sleep efficiency (%)	93.0 (4.7)	97.1 (3.1)	−3.46	<0.01
$Delta_{2\ h}$ (uV^2/min)	1340 (275)	1495 (312)	−3.108	<0.01

Data are expressed as mean (standard deviation) values; SC, sleep control; SD, sleep debt; SWS, slow wave sleep.
$SWS_{2\ h}$, slow wave sleep of first 2 h from sleep onset; $Delta_{2\ h}$, Delta wave power (0.5–4 Hz) of first 2 h from sleep onset.
Degrees of freedom (df) = 13.
doi:10.1371/journal.pone.0056578.t002

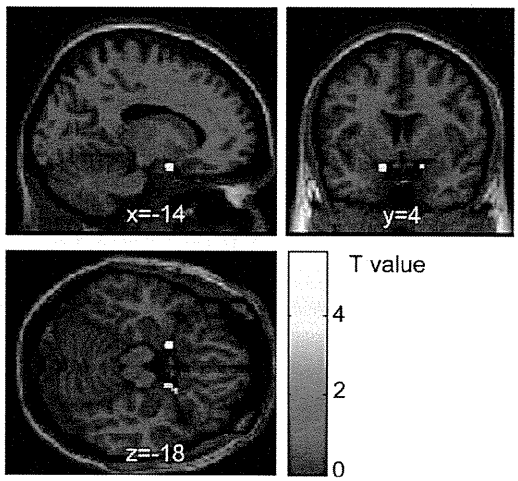

Figure 3. Difference in amygdala activation between the sleep control (SC) and sleep debt (SD) sessions. The map shows significantly greater activation in response to fearful face stimuli in the SD than SC session. Significant differences were seen in the left amygdala, peak MNI coordinate (x, y, z) = (−14, 4, −18) mm, $T(13) = 5.60$, $p = .0001$, $k = 8$ contiguous voxels. A similar trend was also observed in the right amygdala, (x, y, z) = (18, 2, −18) mm, $T(13) = 3.41$, $p = .0005$, $k = 7$. Significant clusters are rendered on a T1 anatomical referential image displayed in neurological convention, with the left side corresponding to the left hemisphere. The clusters shown are thresholded with a lenient alpha level ($p<0.01$, $k>5$) for visualization purposes. MNI, Montreal Neurological Institute template.
doi:10.1371/journal.pone.0056578.g003

$t(13) = -3.05$; right amygdala, x = 24, y = −4, z = −12, $t(13) = -3.08$] or happy vs. neutral contrasts [left amygdala; x = −22, y = −8, z = −14, $t(13) = -2.26$; right amygdala, x = 26, y = −6, z = −16, $t(13) = -2.60$].

We performed the analysis of functional connectivity using only the conscious and fear conditions that showed differential activation between the SD and SC sessions.

fMRI functional connectivity

Comparative analysis of fear vs. neutral contrasts for the conscious condition revealed that, compared with the SC session, $FC_{amg\text{-}vACC}$ was significantly diminished in the SD session [x = 14, y = 32, z = −4, $t(13) = 4.77$] (Fig. 4; Table 3).

Analysis of all of the task results from the SD and SC sessions showed a significantly negative correlation between the activation of left amygdala and $FC_{amg\text{-}vACC}$ [$r(13) = 0.63$, $p<0.001$] (Fig. 5).

Correlations between mood/sleep changes and fMRI data

Sleep debt-related cross-correlation between left amygdala activation, $FC_{amg\text{-}vACC}$, and changes in mood and sleep states are shown in Table 4. Changes of $FC_{amg\text{-}vACC}$ between sessions ($\Delta FC_{amg\text{-}vACC}$) were negatively correlated with the changes of degree of sleep debt ($\Delta SWS_{2\ h}$ and $\Delta\delta_{2\ h}$) as well as mood changes (ΔSTAI-S (Fig. 6), ΔPOMS Tension-Anxiety, and ΔPOMS Confusion). On the other hand, no significant correlations were observed between Δamygdala activation and any of the parameters of the changes in mood or sleep states.

Discussion

The results of this study revealed that sleep debt caused by having just a few hours of sleep for 5 days (3 h 29 min/day of sleep restriction compared with the SC session) increased the activity of the left amygdala in response to a fear facial image. In contrast, a happy facial image did not change the activity. Functional connectivity analysis demonstrated that the levels of $FC_{amg\text{-}vACC}$ (left amygdala-vACC functional connectivity) were lower in participants with higher degrees of sleep debt ($\Delta SWS_{2\ h}$ and $\Delta\delta_{2\ h}$). The most important and novel finding in this paper is that declines in $FC_{amg\text{-}vACC}$ were correlated with left amygdala activation and subjective mood deterioration (higher STAI-S and POMS scores). These findings strongly suggest that down-regulation of the amygdala by the vACC and subsequent activation of the amygdala in response to negative emotional stimuli are involved in intensified physiological and psychological responses [10,11,12] and mood deterioration [13,28] due to unpleasant emotional stimuli during sleep debt.

This interpretation is supported by a series of studies. The amygdala is thought to play an important role in the expression of negative emotions [43,44,45]. Facial expressions of fear were found to activate the amygdala even in healthy individuals with normal sleep [46,47], and such activation is reportedly more prominent in individuals with depression and anxiety disorders [48,49,50]. Moreover, the amygdala has a strong functional and anatomical connection with the mPFC region [51], and the strength of this functional connection is correlated with the degree of subjective emotional suppression and reappraisal of negative affect. [12,52,53].

According to previous studies [12,14], overnight total sleep deprivation diminishes the functional connectivity between the amygdala and the mPFC. In the present study, even a short-term, continuous and accumulating sleep debt that can occur in everyday life clearly resulted in reduced functional connectivity between the amygdala and the mPFC, and more specifically the vACC.

Table 3. Anatomical coordinates for regions of significant difference between the sleep control and sleep deprivation session compared with fear vs. neutral contrast.

Area		BA	MNI x	y	z	*t*	Z	*p*	Cluster k*
SD>SC Activity in amygdala mask									
Left	Amygdala	34	−14	4	−18	5.6	3.93	<0.001	9
SC>SD Functional connectivity with amygdala in ACC/MPFC mask									
Right	Anterior Cingulate	32	14	32	−4	4.77	3.56	<0.001	9

SC, sleep control session; SD, sleep debt session.
Cluster k* $p<0.001$ uncorrected threshold.
Degrees of freedom (df) = 13.
doi:10.1371/journal.pone.0056578.t003

More importantly, subjective mood changes (increased anxiety) following short sleep were correlated with diminished $FC_{amg\text{-}vACC}$, but not with the change in the activation in the amygdala (Δamygdala activation) itself. This may indicate that diminished synchronization between the amygdala and the vACC plays a more important role than the extent of the event-related local activation in the amygdala, for stabilizing increased anxiety evoked by an unpleasant emotional stimulus. Some models of amygdala functionality [53,54] suggest that the magnitude of the local activity in the amygdala does not play a direct role in modulating the mood states of individuals, but the functional connectivity between the amygdala and the ventral mPFC correlates with STAI state score during resting state fMRI [55]. In our functional connectivity analysis, the main event-related hemodynamic response covaries with the seed-related (amygdala) activity in the GLM model of functional connectivity analysis; namely, main event-related immediate reactivity was regressed in our functional connectivity results (see Friston et al., 1997 [42] for the detailed process). Therefore, $FC_{amg\text{-}vACC}$ in this study does not include simple event-related 'co-activation' between two regions, but finer event-unrelated synchronization between two regions beyond the local activities in two regions. This is why the local amygdala activity and the functional connectivity did not correlate with the psychological measurements in the same way; namely, the sustained anxiety (mood) state correlated with the $FC_{amg\text{-}vACC}$, but not with the event-related local reactivity of the amygdala. This interpretation is supported by the diminished functional connectivity between the amygdala and the vACC or ventral mPFC, regardless of the amygdala's activity, in individuals with social anxiety disorder, in those with the s allele of the serotonin transporter gene and who thus have a high risk of depression, and in those with schizophrenia [56,57,58].

Although it has been shown that positive emotional stimuli also activate the amygdala [54,55], happy facial expressions did not significantly alter amygdala activity during sleep debt in the present study. This suggests that functional changes in the amygdala and $FC_{amg\text{-}vACC}$ during sleep debt become more apparent when negative emotional stimuli are presented. Overnight total sleep deprivation reportedly induces activation of the

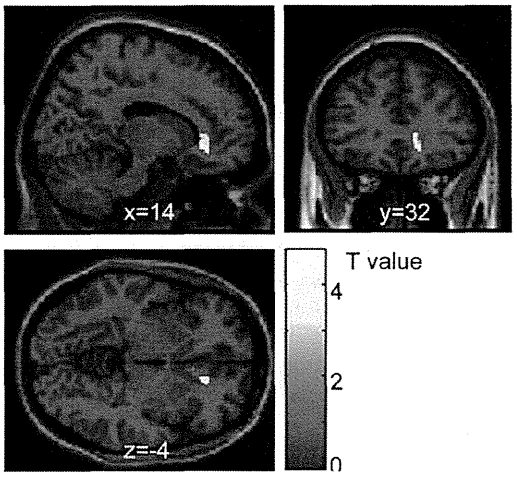

Figure 4. Difference in functional connectivity between sleep control (SC) and sleep debt (SD) sessions. The map shows greater functional connectivity between the left amygdala and other voxels in the brain in SC than SD session. Significant differences were found in the vACC, peak MNI coordinate (*x*, *y*, *z*) = (14, 32, −4) mm, $T(13) = 4.77$, $p = .0001$, $k = 9$ contiguous voxels. The significant cluster with a stronger connection with the left amygdala is rendered on a T1 anatomical referential image displayed in neurological convention, with the left side corresponding to the left hemisphere. The clusters shown are thresholded with a lenient alpha level ($p<0.01$, $k>5$) for visualization purposes. MNI, Montreal Neurological Institute template; vACC, ventral anterior cingulate cortex.
doi:10.1371/journal.pone.0056578.g004

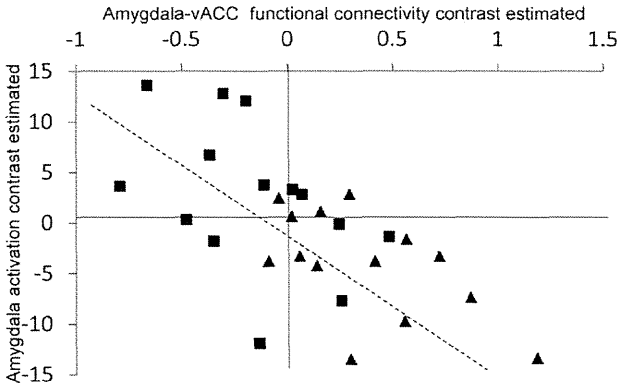

Figure 5. Correlation between amygdala activation and amygdala–vACC functional connectivity. Amygdala activation in response to fearful facial stimuli was negatively correlated with amygdala-vACC functional connectivity, $r(13) = .64$, $p = .0001$. The selected seed region within the amygdala was a cluster that showed greater functional connectivity with vACC in the SC than SD condition ($p<0.001$, uncorrected). Data from the SC and SD sessions were combined and plotted in one graph but differently colored; SD data in squares, SC in triangles. vACC, ventral anterior cingulate cortex; SC, sleep control condition; SD, sleep debt condition.
doi:10.1371/journal.pone.0056578.g005

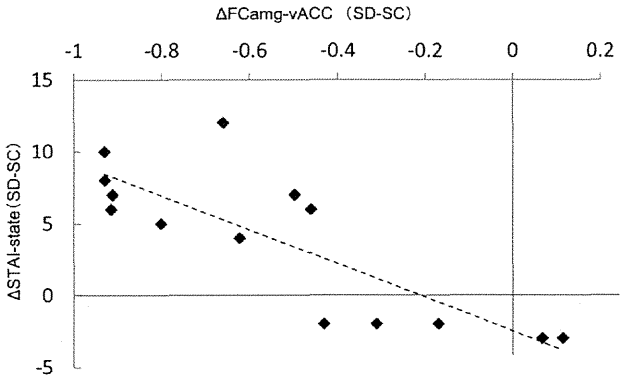

Figure 6. Correlation between the inter-session differences of amygdala–vACC functional connectivity and the inter-session differences STAI-state score. Inter-session differences between sleep control and sleep debt sessions of amygdala-vACC functional connectivity in response to fearful facial stimuli correlated negatively with inter-session differences of STAI-state score, $r(13) = .82$, $p = .0001$. Δvalue, inter-session difference between sleep control and sleep debt sessions for each value; vACC, ventral anterior cingulate cortex; SC, sleep control condition; SD, sleep debt condition; $FC_{amg\text{-}vACC}$, functional connectivity between amygdala and ventral ACC; STAI, State-Trait Anxiety Inventory.
doi:10.1371/journal.pone.0056578.g006

amygdala even in response to images associated with positive emotions [56]. It is reasonable to assume that this discrepancy is due to differences in the sleep conditions, such as total sleep deprivation in the former study and 5-day sleep restriction in the present one. It is possible that overnight sleep deprivation, more than accumulating sleep debt, affects the expression of positive emotion. In fact, overnight sleep deprivation elicits an antidepressant effect in patients with depression, as well as mood activation in healthy individuals [57,58,59,60,61]. Such effect and mood activation might be related to enhanced amygdala activation to positive emotional stimulus, as observed in a previous study. This notion is supported by the findings of a study in which antidepressant treatment enhanced amygdala activation in response to happy faces in patients with depression [62]. However, no similar phenomena have been reported in individuals with consecutive nights of sleep loss.

Unexpectedly, the presentation of emotional facial images under the non-conscious condition did not elicit changes in the amygdala activation after sleep restriction in the present study. A previous study showed that responses to masked priming are enhanced after a 2-day partial sleep deprivation [15]. Moreover, overnight total sleep deprivation strengthened the functional connectivity of amygdala with the sub-cortical region (midbrain) while diminishing the functional connectivity with the mPFC [14]. Based on these findings, we had expected to observe certain functional alteration in not only conscious processing through the cortical pathway, but also non-conscious processing through the subcortical pathway. However, no such alteration was observed in our participants. Any changes in non-conscious processing might be observable by adjusting the length of non-conscious image presentation, the intensity of the facial image stimuli, or increasing the sample size.

Interestingly, the decline in $FC_{amg\text{-}vACC}$ was correlated with the increase in %SWS and δ wave power in the early period of the sleep, but not with subjective sleepiness. Because the increase in SWS and δ wave power is thought to be a sensitive indicator of the sleep homeostatic process [63,64], it is possible that $FC_{amg\text{-}vACC}$ is

Table 4. Correlations between inter-session differences for fMRI data and questionnaire scores, and objective sleep debt Indices.

	ΔAmygdala activation	$\Delta FC_{amg\text{-}vACC}$
ΔSTAI-state	0.02	−0.82***
ΔPOMS Vigor	−0.22	0.49
ΔPOMS Depression	−0.20	−0.46
ΔPOMS Anger-Hostility	−0.38	0.11
ΔPOMS Fatigue	−0.27	−0.28
ΔPOMS Tension-Anxiety	0.13	−0.73**
ΔPOMS Confusion	0.02	−0.60*
ΔSSS	−0.41	0.01
$\Delta SWS_{2\ hrs}$	0.36	−0.59*
$\Delta Delta_{2\ hrs}$	0.03	−0.55*

Note. Δvalue, inter-session difference between sleep control and sleep debt sessions for each value; $FC_{amg\text{-}vACC}$, functional connectivity between amygdala and ventral ACC; SSS, Stanford Sleepiness Scale; STAI, State-Trait Anxiety Inventory; POMS, Profile of Mood States; $SWS_{2\ h}$, slow wave sleep of first 2 h from sleep onset; $Delta_{2\ h}$, delta wave power of first 2 h from sleep onset;
*$p<0.05$,
**$p<0.01$,
***$p<0.001$.
Degrees of freedom (df) = 13.
doi:10.1371/journal.pone.0056578.t004

associated with the neural basis that enhances homeostatic sleep pressure following short hours of sleep. It is also thought that the increase in homeostatic sleep pressure is caused by the accumulation of sleep promoting substances in brain, such as prostaglandin D2 and adenosine [65,66,67,68,69]. For example, adenosine receptor antagonists have been shown to reduce sleep time by increasing wake hours and reduce slow wave activity during sleep [65,66,68]. Recent studies have hypothesized that adenosine, accumulated in the synaptic cleft because of consecutive synaptic transmission, binds to the A1 receptor to suppress synaptic transmission [70]. It is possible that synaptic suppression by a sleep-promoting substance is involved in the attenuation of $FC_{amg\text{-}vACC}$ during sleep debt. Functional connectivity of the BOLD signal reportedly reflects a synaptic anatomical pathway [71]; therefore, it is expected that synaptic suppression by adenosine causes a decline in functional connectivity. This hypothesis is supported by a previous study which reported that a lack of sleep leads to attenuated resting state functional connectivity [72]. Moreover, a positron emission tomography (PET) study of human subjects revealed increased adenosine binding to the A1 receptor in regions including the vACC during sleep deprivation [73]. The use of PET with fMRI to elucidate the effects of sleep-promoting substances such as adenosine, including the effect of adenosine on the dynamics of neural activity in the brain, will likely elucidate the neural basis that alters the mechanism of emotion regulation.

Some limitations need to be taken into account when interpreting the present findings. First, participants in this study spent the first 3 days at home. Even though their sleep schedule was enforced by the use of the actigraph and mail alerts, their actual sleep time (8 h 5 min and 4 h 36 min in the SC and SD session, respectively) was longer than the scheduled sleep time (8 and 4 h in the SC and SD session, respectively). Despite the minor increase in sleep time, the SD session had a sleep loss of 3 h 30 min compared with the SC session. This level of sleep loss is rather frequently experienced in everyday life; however, the presence of sleep debt was confirmed on the last day of the session

by the increase in %SWS and δ wave power. Because sleep requirements vary among individuals, the same sleep schedule may result in large individual differences in sleep debt [74]. In other words, even if everyone were to be placed strictly on the same sleep schedule, the effects of sleep debt on brain activity and subjective moods would vary widely among individuals. If sleep can be restricted based on individual sleep requirements, functional changes in the amygdala and $FC_{amg\text{-}vACC}$ might be identified more accurately.

Conclusion

The results of this study indicate that a short-term sleep loss, which is often experienced in everyday life, can aggravate subjective mood including anxiety, and the mechanism appears to involve functional alteration of the amygdala and $FC_{amg\text{-}vACC}$. Long work hours, night-owl lifestyles, and an increase in shift work are the major contributors to sleep loss and thus the risk for depression [1,2,4,6,75,76,77,78]. Therefore, ensuring adequate sleep is an important lifestyle factor that deserves more attention in terms of managing mental health, including depression.

Acknowledgments

We would like to thank all the staff at the Department of Psychophysiology, National Institute of Mental Health, National Center of Neurology and Psychiatry for facilitating the completion of this study.

Author Contributions

Conceived and designed the experiments: Y. Motomura SK KO YT Y. Moriguchi KM. Performed the experiments: Y. Motomura SK KO YT ME YK AH. Analyzed the data: Y. Motomura SK ME. Contributed reagents/materials/analysis tools: Y. Motomura SK KO YT ME Y. Moriguchi. Wrote the paper: Y. Motomura SK Y. Moriguchi SH KM.

References

1. Basner M, Fomberstein KM, Razavi FM, Banks S, William JH, et al. (2007) American time use survey: sleep time and its relationship to waking activities. Sleep 30: 1085–1095.
2. Bonnet MH, Arand DL (1995) We are chronically sleep deprived. Sleep 18: 908–911.
3. Breslau N, Roth T, Rosenthal L, Andreski P (1997) Daytime sleepiness: an epidemiological study of young adults. Am J Public Health 87: 1649–1653.
4. Hublin C, Kaprio J, Partinen M, Koskenvuo M (2001) Insufficient sleep–a population-based study in adults. Sleep 24: 392–400.
5. Kaneita Y, Ohida T, Uchiyama M, Takemura S, Kawahara K, et al. (2005) Excessive daytime sleepiness among the Japanese general population. J Epidemiol 15: 1–8.
6. Rajaratnam SMW, Arendt J (2001) Health in a 24-h society. The Lancet 358: 999–1005.
7. Carskadon MA, Dement WC (1981) Cumulative effects of sleep restriction on daytime sleepiness. Psychophysiology 18: 107–113.
8. Chuah LY, Chee MW (2008) Functional neuroimaging of sleep deprived healthy volunteers and persons with sleep disorders: a brief review. Ann Acad Med Singapore 37: 689–694.
9. Durmer JS, Dinges DF (2005) Neurocognitive consequences of sleep deprivation. Seminars in Neurology 25: 117–129.
10. Franzen PL, Buysse DJ, Dahl RE, Thompson W, Siegle GJ (2009) Sleep deprivation alters pupillary reactivity to emotional stimuli in healthy young adults. Biol Psychol 80: 300–305.
11. Zhong X, Hilton HJ, Gates GJ, Jelic S, Stern Y, et al. (2005) Increased sympathetic and decreased parasympathetic cardiovascular modulation in normal humans with acute sleep deprivation. J Appl Physiol 98: 2024–2032.
12. Chuah LY, Dolcos F, Chen AK, Zheng H, Parimal S, et al. (2010) Sleep deprivation and interference by emotional distracters. Sleep 33: 1305–1313.
13. Minkel JD, Banks S, Htaik O, Moreta MC, Jones CW, et al. (2012) Sleep Deprivation and Stressors: Evidence for Elevated Negative Affect in Response to Mild Stressors When Sleep Deprived. Emotion 12: 1015–1020.
14. Yoo S-S, Gujar N, Hu P, Jolesz FA, Walker MP (2007) The human emotional brain without sleep — a prefrontal amygdala disconnect. Current Biology 17: R877–R878.
15. Swann CE, Yelland GW, Redman JR, Rajaratnam SM (2006) Chronic partial sleep loss increases the facilitatory role of a masked prime in a word recognition task. J Sleep Res 15: 23–29.
16. Killgore WD, Yurgelun-Todd DA (2004) Activation of the amygdala and anterior cingulate during nonconscious processing of sad versus happy faces. Neuroimage 21: 1215–1223.
17. Morris JS, Ohman A, Dolan RJ (1999) A subcortical pathway to the right amygdala mediating "unseen" fear. Proc Natl Acad Sci U S A 96: 1680–1685.
18. Nomura M, Ohira H, Haneda K, Iidaka T, Sadato N, et al. (2004) Functional association of the amygdala and ventral prefrontal cortex during cognitive evaluation of facial expressions primed by masked angry faces: an event-related fMRI study. Neuroimage 21: 352–363.
19. Pessoa L, Adolphs R (2010) Emotion processing and the amygdala: from a 'low road' to 'many roads' of evaluating biological significance. Nat Rev Neurosci 11: 773–783.
20. Whalen PJ, Rauch SL, Etcoff NL, McInerney SC, Lee MB, et al. (1998) Masked presentations of emotional facial expressions modulate amygdala activity without explicit knowledge. J Neurosci 18: 411–418.
21. Etkin A, Klemenhagen KC, Dudman JT, Rogan MT, Hen R, et al. (2004) Individual Differences in Trait Anxiety Predict the Response of the Basolateral Amygdala to Unconsciously Processed Fearful Faces. Neuron 44: 1043–1055.
22. Williams LM, Das P, Liddell BJ, Kemp AH, Rennie CJ, et al. (2006) Mode of functional connectivity in amygdala pathways dissociates level of awareness for signals of fear. J Neurosci 26: 9264–9271.
23. Banks S, Dinges DF (2007) Behavioral and physiological consequences of sleep restriction. J Clin Sleep Med 3: 519–528.
24. Banks S, Van Dongen H, Dinges DF (2010) Effect of Sleep Dose on Recovery Sleep Stage and Slow Wave Energy Dynamics Following Chronic Sleep Restriction. Sleep 33: A104–A104.
25. Belenky G, Wesensten NJ, Thorne DR, Thomas ML, Sing HC, et al. (2003) Patterns of performance degradation and restoration during sleep restriction and subsequent recovery: a sleep dose-response study. Journal of Sleep Research 12: 1–12.
26. Dinges DF, Pack F, Williams K, Gillen KA, Powell JW, et al. (1997) Cumulative sleepiness, mood disturbance, and psychomotor vigilance performance decrements during a week of sleep restricted to 4–5 hours per night. Sleep 20: 267–277.
27. Van Dongen HP, Maislin G, Mullington JM, Dinges DF (2003) The cumulative cost of additional wakefulness: dose-response effects on neurobehavioral functions and sleep physiology from chronic sleep restriction and total sleep deprivation. Sleep 26: 117–126.
28. Zohar D, Tzischinsky O, Epstein R, Lavie P (2005) The effects of sleep loss on medical residents' emotional reactions to work events: a cognitive-energy model. Sleep 28: 47–54.
29. Cole RJ, Kripke DF, Gruen W, Mullaney DJ, Gillin JC (1992) Automatic sleep/wake identification from wrist activity. Sleep 15: 461–469.
30. Ekman P, Friesen WV (1971) Constants across cultures in the face and emotion. J Pers Soc Psychol 17: 124–129.
31. Ogawa T, Oda M, Yoshikawa S, Akamatsu S (1997) Evaluation of Facial Expressions Differing in Face Angles: Constructing a Database of Facial Expressions. The Institute of Electronics, Information and Communication Engineers, technical report, HIP, Human Information Processing 97: 47–52.
32. Hoddes E, Zarcone V, Smythe H, Phillips R, Dement WC (1973) Quantification of sleepiness: a new approach. Psychophysiology 10: 431–436.
33. Spielberger CD, Gorsuch RL (1970) STAI Manual for the Stait-Trait Anxiety Inventory.
34. McNair DM, Lorr M, Droppleman LF (1971) Profile of Mood States (POMS™).
35. Rechtschaffen A, Kales A (1968) A manual of standardized terminology, techniques and scoring system for sleep stages of human subjects(National Institutes of Health).
36. Agnew HW, Jr., Webb WB, Williams RL (1966) The first night effect: an EEG study of sleep. Psychophysiology 2: 263–266.
37. Akerstedt T, Kecklund G, Ingre M, Lekander M, Axelsson J (2009) Sleep homeostasis during repeated sleep restriction and recovery: support from EEG dynamics. Sleep 32: 217–222.
38. Borbely AA, Achermann P (1999) Sleep homeostasis and models of sleep regulation. J Biol Rhythms 14: 557–568.
39. Brunner DP, Dijk DJ, Borbely AA (1993) Repeated partial sleep deprivation progressively changes in EEG during sleep and wakefulness. Sleep 16: 100–113.
40. Dijk DJ, Hayes B, Czeisler CA (1993) Dynamics of electroencephalographic sleep spindles and slow wave activity in men: effect of sleep deprivation. Brain Res 626: 190–199.
41. Worsley KJ, Marrett S, Neelin P, Vandal AC, Friston KJ, et al. (1996) A unified statistical approach for determining significant signals in images of cerebral activation. Hum Brain Mapp 4: 58–73.
42. Friston KJ, Buechel C, Fink GR, Morris J, Rolls E, et al. (1997) Psychophysiological and modulatory interactions in neuroimaging. Neuroimage 6: 218–229.

43. Gloor P, Olivier A, Quesney LF, Andermann F, Horowitz S (1982) The role of the limbic system in experiential phenomena of temporal lobe epilepsy. Ann Neurol 12: 129–144.
44. Halgren E, Walter RD, Cherlow DG, Crandall PH (1978) Mental phenomena evoked by electrical stimulation of the human hippocampal formation and amygdala. Brain 101: 83–117.
45. Phelps EA (2006) Emotion and cognition: insights from studies of the human amygdala. Annu Rev Psychol 57: 27–53.
46. Fitzgerald DA, Angstadt M, Jelsone LM, Nathan PJ, Phan KL (2006) Beyond threat: amygdala reactivity across multiple expressions of facial affect. Neuroimage 30: 1441–1448.
47. Fusar-Poli P, Placentino A, Carletti F, Landi P, Allen P, et al. (2009) Functional atlas of emotional faces processing: a voxel-based meta-analysis of 105 functional magnetic resonance imaging studies. Journal of Psychiatry & Neuroscience 34: 418–432.
48. Dannlowski U, Ohrmann P, Bauer J, Kugel H, Baune BT, et al. (2007) Serotonergic genes modulate amygdala activity in major depression. Genes Brain Behav 6: 672–676.
49. McClure EB, Monk CS, Nelson EE, Parrish JM, Adler A, et al. (2007) Abnormal attention modulation of fear circuit function in pediatric generalized anxiety disorder. Arch Gen Psychiatry 64: 97–106.
50. Sheline YI, Barch DM, Donnelly JM, Ollinger JM, Snyder AZ, et al. (2001) Increased amygdala response to masked emotional faces in depressed subjects resolves with antidepressant treatment: An fMRI study. Biological Psychiatry 50: 651–658.
51. Kim MJ, Loucks RA, Palmer AL, Brown AC, Solomon KM, et al. (2011) The structural and functional connectivity of the amygdala: From normal emotion to pathological anxiety. Behavioural Brain Research 223: 403–410.
52. Banks SJ, Eddy KT, Angstadt M, Nathan PJ, Phan KL (2007) Amygdala-frontal connectivity during emotion regulation. Soc Cogn Affect Neurosci 2: 303–312.
53. Urry HL, van Reekum CM, Johnstone T, Kalin NH, Thurow ME, et al. (2006) Amygdala and ventromedial prefrontal cortex are inversely coupled during regulation of negative affect and predict the diurnal pattern of cortisol secretion among older adults. J Neurosci 26: 4415–4425.
54. Hampton AN, Adolphs R, Tyszka MJ, O'Doherty JP (2007) Contributions of the amygdala to reward expectancy and choice signals in human prefrontal cortex. Neuron 55: 545–555.
55. Murray EA (2007) The amygdala, reward and emotion. Trends Cogn Sci 11: 489–497.
56. Gujar N, Yoo SS, Hu P, Walker MP (2011) Sleep deprivation amplifies reactivity of brain reward networks, biasing the appraisal of positive emotional experiences. J Neurosci 31: 4466–4474.
57. Bliss EL, Clark LD, West CD (1959) Studies of sleep deprivation-relationship to schizophrenia. AMA Arch Neurol Psychiatry 81: 348–359.
58. Dahl RE (2004) Regulation of sleep and arousal: comments on part VII. Ann N Y Acad Sci 1021: 292–293.
59. Gillin JC, Buchsbaum M, Wu J, Clark C, Bunney W, Jr. (2001) Sleep deprivation as a model experimental antidepressant treatment: findings from functional brain imaging. Depress Anxiety 14: 37–49.
60. Horne JA (1993) Human sleep, sleep loss and behaviour. Implications for the prefrontal cortex and psychiatric disorder. Br J Psychiatry 162: 413–419.
61. Wirz-Justice A, Van den Hoofdakker RH (1999) Sleep deprivation in depression: what do we know, where do we go? Biol Psychiatry 46: 445–453.
62. Norbury R, Taylor MJ, Selvaraj S, Murphy SE, Harmer CJ, et al. (2009) Short-term antidepressant treatment modulates amygdala response to happy faces. Psychopharmacology (Berl) 206: 197–204.
63. Achermann P, Dijk DJ, Brunner DP, Borbely AA (1993) A model of human sleep homeostasis based on EEG slow-wave activity: quantitative comparison of data and simulations. Brain Res Bull 31: 97–113.
64. Borbely AA, Baumann F, Brandeis D, Strauch I, Lehmann D (1981) Sleep deprivation: effect on sleep stages and EEG power density in man. Electroencephalogr Clin Neurophysiol 51: 483–495.
65. Basheer R, Strecker RE, Thakkar MM, McCarley RW (2004) Adenosine and sleep-wake regulation. Prog Neurobiol 73: 379–396.
66. Benington JH, Heller HC (1995) Restoration of brain energy metabolism as the function of sleep. Prog Neurobiol 45: 347–360.
67. Krueger JM, Rector DM, Roy S, Van Dongen HP, Belenky G, et al. (2008) Sleep as a fundamental property of neuronal assemblies. Nat Rev Neurosci 9: 910–919.
68. Landolt HP (2008) Sleep homeostasis: a role for adenosine in humans? Biochem Pharmacol 75: 2070–2079.
69. Urade Y, Hayaishi O (2011) Prostaglandin D2 and sleep/wake regulation. Sleep Med Rev 15: 411–418.
70. Jones BE (2009) Glia, adenosine, and sleep. Neuron 61: 156–157.
71. Lu J, Liu H, Zhang M, Wang D, Cao Y, et al. (2011) Focal pontine lesions provide evidence that intrinsic functional connectivity reflects polysynaptic anatomical pathways. J Neurosci 31: 15065–15071.
72. Killgore WDS, Schwab ZJ, Weiner MR (2012) Self-reported nocturnal sleep duration is associated with next-day resting state functional connectivity. Neuroreport 23: 741–745.
73. Elmenhorst D, Meyer PT, Winz OH, Matusch A, Ermert J, et al. (2007) Sleep deprivation increases A1 adenosine receptor binding in the human brain: a positron emission tomography study. J Neurosci 27: 2410–2415.
74. Van Dongen HP, Baynard MD, Maislin G, Dinges DF (2004) Systematic interindividual differences in neurobehavioral impairment from sleep loss: evidence of trait-like differential vulnerability. Sleep 27: 423–433.
75. Chalupka S (2012) Overtime Work as a Predictor of a Major Depressive Episode. Workplace Health & Safety 60: 192–192.
76. Kitamura S, Hida A, Watanabe M, Enomoto M, Aritake-Okada S, et al. (2010) Evening preference is related to the incidence of depressive states independent of sleep-wake conditions. Chronobiol Int 27: 1797–1812.
77. Scott AJ, Monk TH, Brink LL (1997) Shiftwork as a Risk Factor for Depression: A Pilot Study. Int J Occup Environ Health 3: S2–S9.
78. Virtanen M, Stansfeld SA, Fuhrer R, Ferrie JE, Kivimaki M (2012) Overtime Work as a Predictor of Major Depressive Episode: A 5-Year Follow-Up of the Whitehall II Study. Plos One 7.

Neuropsychiatric Disease and Treatment

Dovepress

open access to scientific and medical research

Open Access Full Text Article

ORIGINAL RESEARCH

Clozapine-induced seizures, electroencephalography abnormalities, and clinical responses in Japanese patients with schizophrenia

This article was published in the following Dove Press journal:
Neuropsychiatric Disease and Treatment
15 October 2014
Number of times this article has been viewed

Yuka Sugawara Kikuchi
Wataru Sato
Keiichiro Ataka
Kiwamu Yagisawa
Yuki Omori
Takashi Kanbayashi
Tetsuo Shimizu

Department of Neuropsychiatry, Akita University Graduate School of Medicine, Hondo, Akita, Japan

Purpose: We describe electroencephalography (EEG) abnormalities and seizures associated with clozapine treatment in Japanese patients with schizophrenia and retrospectively compare EEG results and total Positive and Negative Syndrome Scale (PANSS [T]) scores before and after treatment.

Methods: Twenty-six patients with treatment-resistant schizophrenia were enrolled in this study. EEG measurements were obtained prior to clozapine treatment and every 4 weeks thereafter. EEG measurements were also obtained at the time of seizure. After seizures or EEG abnormalities were noted, additional EEGs were performed every 2 weeks. PANSS (T) scores were used to determine clozapine treatment outcome.

Results: All 26 patients had normal baseline EEG measurements, and ten patients (38.5%) later manifested EEG abnormalities. The mean age was significantly lower than in the abnormal EEG group. Six patients (23.1%) experienced seizures. The mean dose of clozapine at the first occurrence of seizure was 383.3 mg/day. Five of six patients who experienced seizures in this study were successfully treated with valproate or lamotrigine without discontinuation of clozapine. The one patient who continued to experience seizures was successfully treated without antiepileptic drugs. The mean baseline PANSS (T) scores were not significantly different between the normal and abnormal EEG groups, but the mean score in the abnormal EEG group was significantly lower than that in the normal EEG group at the final follow-up (P=0.02).

Conclusion: EEG abnormalities may appear in younger patients, and our findings indicate that there is no need to discontinue clozapine when seizures occur. EEG abnormalities that appeared after clozapine treatment were associated with a good clinical response.

Keywords: treatment-resistant schizophrenia, side effects, PANSS, convulsions

Introduction

Despite pharmacological advances, about 10%–30% of patients with schizophrenia exhibit little or no response to antipsychotic medications, and persistent symptoms make it difficult for these patients to re-enter society. Clozapine is effective against treatment-resistant schizophrenia (TRS) and was introduced to Japan in 2009. In Japan, all physicians who prescribe clozapine, as well as the patients receiving the drug, must be registered with the Clozaril Patient Monitoring Service (CPMS). In addition, clozapine is limited to patients with TRS according to the following poor response and poor tolerance criteria. The poor response criterion is a failure to respond to a sufficient term (at least 4 weeks) of treatment with a sufficient dose of at least two well-tolerated antipsychotics (including at least one atypical antipsychotic [eg, risperidone, perospirone, olanzapine, quetiapine, or aripiprazole at over 600 mg/day chlorpromazine equivalent]). The poor tolerance criterion is defined as a failure to adequately respond to monotherapy with at least two atypical antipsychotics (eg, risperidone perospirone, olanzapine, quetiapine, and aripiprazole) due to failure to increase the dose to a necessary level for any of the

Correspondence: Yuka Sugawara Kikuchi
Department of Neuropsychiatry, Akita University Graduate School of Medicine, 1-1-1 Hondo, Akita 010-8543, Japan
Tel +81 18 884 6122
Fax +81 18 884 6445
Email yuka@med.akita-u.ac.jp

submit your manuscript www.dovepress.com
Dovepress
http://dx.doi.org/10.2147/NDT.S69784

following reasons: occurrence or worsening of moderate or severe tardive dyskinesia, tardive dystonia, or other tardive extrapyramidal symptoms, or occurrence of uncontrolled parkinsonian symptoms, akathisia, or acute dystonia.

Clozapine also causes serious side effects, such as agranulocytosis and seizures. Clozapine-induced seizures are more frequent than agranulocytosis,[1] and electroencephalography (EEG) abnormalities are even more common. The appearance of paroxysmal discharges indicates a high risk for convulsion.[2] However, EEG abnormalities that develop after clozapine treatment appear to be associated with good responses.[3] Herein, we describe EEG abnormalities and seizures associated with clozapine treatment in Japanese patients with schizophrenia and retrospectively compare EEG results and total Positive and Negative Syndrome Scale (PANSS [T]) scores before and after treatment.

Materials and methods

Subjects and demographic profiles

The subjects were all consecutive hospitalized patients with TRS. All patients met the criteria of poor response or poor tolerance described above. No patient had received clozapine before or had a history of prior seizure or brain injury. Twenty-eight patients were recruited in this study, but two patients were excluded because clozapine was discontinued when they developed side effects before post-treatment EEG measurement. One patient developed cardiomyopathy 4 weeks after starting clozapine, and the other developed agranulocytosis 3 weeks after initiating clozapine. Ultimately, 26 patients (eight males, 18 females) with an average age of 37 years were enrolled. Clozapine was initiated at a starting dose of 12.5 mg/day on the first day and was increased to 25 mg/day on the second day. On the third day and thereafter, the daily dose could be slowly increased in 25 mg increments to achieve a dose of up to 200 mg/day over 3 weeks. The dose was increased depending on the symptoms; however, at least 4 days were required to pass for dose increases in increments of up to 100 mg. The maximum dose in Japan is 600 mg/day. In principle, the duration of hospitalization was defined as 18 weeks after initiating clozapine according to the manufacturer's specifications (Novartis International AG, Basel, Switzerland). However, as long as certain criteria were met, patients could be discharged before 18 weeks. These criteria were desirable for discharge; achievement of the maintenance dosage, at least 3 weeks' hospitalization, improvement of clinical symptoms, and confirmation of safety.

EEG recording and clinical response

EEG recordings were performed with the use of the International 10–20 system and a 21-channel monitor. The patient's history and medications were blinded to readers who read the EEG recordings. EEG measures were obtained several days prior to the initiation of clozapine treatment, and every 4 weeks thereafter. EEG measures were also obtained immediately after seizures occurred. Following seizures or EEG abnormalities, additional EEGs were performed every 2 weeks. PANSS (T) scores were used to determine clozapine treatment outcomes.

Data analysis

The incidences of seizures and EEG abnormality were obtained, and subjects were divided into two groups depending on whether their EEG recording was normal or abnormal. Student's *t*-tests and chi-square tests were used to compare demographic profiles between the two groups. PANSS (T) scores were compared at baseline and at the last observation with Student's *t*-tests.

Results

Clozapine-induced EEG abnormality

All patients had normal baseline EEG measures, and ten patients (38.5%) later showed EEG abnormalities. The daily dose of clozapine at the occurrence of EEG abnormalities varied from 125 to 600 mg (mean 305 mg/day). There were no significant differences between the normal and abnormal EEG groups in terms of sex, mean dose of clozapine, or length of clozapine treatment (Table 1). In the abnormal EEG group, the mean age and illness duration were significantly lower and shorter, respectively, than the corresponding values in the normal EEG group (Table 1). The time to the occurrence of EEG abnormalities varied from 4 to 52 weeks (mean 14.6 weeks). The clinical courses of the patients with EEG abnormality are summarized in Table 2. The numbers of patients with EEG abnormalities were as follows: spikes in one patient, spike and wave complexes in ten patients, and slow waves in four patients (Table 2). No patients withdrew from the study because of the appearance of EEG abnormalities.

Clozapine-induced seizures

Six patients (23.1%) experienced seizures: one with both tonic–clonic and myoclonic, one with tonic–clonic, and four with myoclonic seizures (Table 2). The daily dose of clozapine at first seizure varied from 300–600 mg (mean 383.3 mg/day), and the time to first seizure varied from 8–23 weeks (mean 12.3 weeks). Five of six patients who experienced seizures in this study were successfully treated with valproate or lamotrigine without discontinuation of clozapine. The persistent seizures in one patient were ultimately controlled without the use of antiepileptic drugs. The clinical courses are summarized in Table 2.